Towards a simple representation of chalk hydrology in land surface modelling

Mostaquimur Rahman[1], Rafael Rosolem[1,2]

[1]Department of Civil Engineering, University of Bristol, Bristol, UK

[2]Cabot Institute, University of Bristol, Bristol, UK

Abstract

Modelling and monitoring of hydrological processes in the unsaturated zone of chalk, a porous medium with fractures, is important to optimize water resources assessment and management practices in the United Kingdom (UK). However, incorporating the processes governing water movement through chalk unsaturated zone in a numerical model is complicated mainly due to the fractured nature of chalk that creates high-velocity preferential flow paths in the subsurface. In general, flow through chalk unsaturated zone is simulated using dual-porosity concept, which often involves calibration of relatively large number of model parameters, potentially undermining applications to large regions. Therefore, this approach may be not be suitable for large-scale land surface modelling applications. In this study, a simplified parameterization, namely the Bulk Conductivity (BC) model is proposed for simulating hydrology in chalk unsaturated zone. This new parameterization is implemented in the Joint UK Land Environment Simulator (JULES) and applied to a study area encompassing the Kennet catchment in the Southern UK. The simulation results are evaluated using field measurements and satellite remote sensing observations of various fluxes and states of the hydrological cycle (e.g., soil moisture, runoff and latent heat flux) at two distinct spatial scales (i.e., point and catchment). The results demonstrate that the inclusion of the BC model in JULES improves simulated land surface mass and energy fluxes over the chalk-dominated Kennet catchment. Therefore, the simple approach described in this

study may be used to incorporate the flow processes through chalk unsaturated zone in large scale land surface modelling applications.

Keywords: Chalk hydrology, macroporosity, land surface model, bulk conductivity model.

1. Introduction

Chalk can be described as a fine-grained porous medium traversed by fractures [*Price et al.*, 1993]. Previous studies showed that the unsaturated zone of the chalk aquifers plays an important role on groundwater recharge in the UK [e.g., *Lee et al.*, 2006; *Ireson et al.*, 2009]. Therefore, both monitoring [e.g., *Bloomfield*, 1997; *Ireson et al.*, 2006] and modelling [e.g., *Bakopoulou*, 2015; *Brouyère*, 2006; *Ireson and Butler*, 2011, 2013; *Sorensen et al.*, 2014] strategies have been adapted previously to understand the governing hydrological processes in the chalk unsaturated zone.

In chalk, the matrix provides porosity and storage capacity, while the fractures greatly enhance permeability [*Van den Daele et al.*, 2007]. Water movement through chalk matrix is slow due to its relatively high porosity (0.3-0.4) and low permeability (10^{-9}-10^{-8} ms^{-1}). A fractured chalk system, in contrast, conducts water at a considerably higher velocity because of relatively high permeability (10^{-5}-10^{-3} ms^{-1}) and low porosity (of the order 10^{-4}) of fractures [*Price et al.*, 1993].

Simulating water flow through the matrix-fracture system of chalk has been the subject of research for some time. Both conceptual [e.g., *Price et al.*, 2000; *Haria et al.*, 2003] and physics-based [e.g., *Mathias et al.*, 2006; *Ireson et al.*, 2009] models have been proposed previously to describe water flow through chalk unsaturated zone. The physics-based models mentioned above were developed based on dual-continua approach and required relatively large number of parameters that were calibrated via inverse modelling using observed soil moisture and matric potential data.

In recent years, representation of chalk has gained attention in land surface modelling. *Gascoin et al.* [2009] applied the Catchment Land Surface Model (CLSM) over the Somme River basin in northern France. A linear reservoir was included in the TOPMODEL based runoff formulation of CLSM to account for the contribution of chalk aquifers to river discharge. *Le Vine et al.* [2016] applied the Joint UK Land Environment Simulator (JULES [*Best et al.*, 2011]) over the Kennet catchment in southern England to evaluate the hydrological limitations of land surface models. In that study, two intersecting Brooks and Corey curves were proposed, which allowed a dual curve soil moisture retention representation for the two distinct flow domains of chalk (i.e., matrix and fracture) in the model. Considering this dual Brooks and Corey curve, a three-dimensional groundwater flow model (ZOOMQ3D [*Jackson and Spink*, 2004]) was coupled to JULES to demonstrate the strong influence of representing chalk hydrology and groundwater dynamics on simulated soil moisture and runoff.

The above mentioned studies illustrate the importance of representing chalk in land surface modelling. However, including chalk hydrology in large-scale land surface modelling using the contemporary dual-porosity concept can be complicated because this approach generally involves relatively large number of parameters. In this context, we propose a new parameterization, namely the Bulk Conductivity (BC) model as a first step towards a simple chalk representation suitable for land surface modelling. The BC model is included in JULES and evaluated at two distinct spatial scales (i.e., point and catchment). At the point-scale, the BC model is evaluated using observed soil moisture data. The proposed model is then applied to the Kennet catchment in the Southern England and the fluxes and states of the hydrological cycle are simulated for multiple years. The simulation results are evaluated using observed latent heat flux (LE) and runoff to assess the performance of the BC model in simulating land surface processes at the catchment scale.

2. A model of flow through chalk unsaturated zone

In this study, the *Bulk Conductivity* (BC) model based on the work by *Zehe et al.* [2001] is incorporated in JULES to represent the flow of water through the fractured chalk unsaturated zone. According to this approach, if the relative saturation (S) exceeds a certain threshold (S_0) at a soil grid, the saturated hydraulic conductivity (K_s) is increased to a bulk saturated hydraulic conductivity (K_{sb}) as follows

$$K_{sb} = K_s + K_s f_m \frac{S-S_0}{1-S_0} \qquad \text{if } S > S_0 \qquad (1)$$

with $S = \frac{\theta-\theta_r}{\theta_s-\theta_r}$

where f_m is a macroporosity factor (-), θ is soil moisture (m^3m^{-3}), θ_s is soil moisture at saturation (m^3m^{-3}), and θ_r is the residual soil moisture (m^3m^{-3}). Note that S ranges from zero in case of completely dry soils to one for fully wet soils.

At the first step of evaluation, the K_s, S_0 and f_m parameters are estimated based on existing literature to assess the performance of the uncalibrated BC model. In this uncalibrated BC model, K_s for chalk matrix is 16 mmd^{-1} according to *Le Vine et al.* [2016] for the catchment investigated in this study (Figure 1). Equation 1 indicates that the onset of water flow through the fracture system of chalk is controlled by the threshold S_0. According to *Wellings and Bell* [1980], water flow through fractures dominates over matrix flow in chalk when the pressure head in soil becomes higher than -0.50 mH_2O. We consider a value of $S_0 = 0.80$ for the uncalibrated BC model, which is based on observed soil moisture-matric potential relationship in the study area (Figure S1).

In *Zehe et al.* [2001], f_m was defined as the ratio of the saturated water flow rate in all macropores in a model element to the corresponding value in soil matrix, which can be determined based on the density and length of fractures at small scales. In addition, f_m has also been considered as a calibration parameter previously [e.g., *Blume*, 2008; *Zehe et al.*, 2013]. In this study, we define f_m as a characteristic soil property reflecting the influence of fractures on soil water movement [*Zehe and Blöschl*, 2004], and estimate it from the relative difference of permeability between chalk matrix and fractured chalk system that can be of the order 10^4-10^6 according to *Price et al.* [1999]. Consequently, we consider a macroporosity factor of $f_m = 10^5$ for the uncalibrated BC model.

In the following step, the BC model parameters are optimized to minimize the differences between the variability of observed and simulated soil moisture. Price et al. [1999] argued that the K_s for chalk matrix is generally around 3-5 mmd^{-1} (3.5-5.8x10^{-5} mms^{-1}). In order to optimize the BC model performance, we consider a range of K_s = 0.8-86 mmd^{-1} (10^{-5}-10^{-3} mms^{-1}) for chalk matrix in this study. As mentioned earlier, *S* is zero for completely dry soils and one in case of fully wet soils. Therefore, we consider a range of 0-1.0 for S_0 to optimize the BC model. For f_m, a range of 10^4-10^6 is considered, which, as discussed earlier, is consistent with the relative difference between the permeability of fractured chalk and chalk matrix according to *Price et al* [1999].

We use the Root Mean Squared Error (RMSE) as the objective function to optimize the BC model parameters [e.g., *Ireson et al.*, 2009]

$$RMSE = \frac{1}{nd}\sum_{1}^{nd}\sqrt{\left(\frac{1}{nt-1}\sum_{2}^{nt}\left(\Delta\theta_{d,t}^{obs} - \Delta\theta_{d,t}^{sim}\right)^2\right)} \qquad (2)$$

where *nd* is the number of soil layers, *nt* is the number of soil moisture observations available for a layer *d*, $\Delta\theta^{obs}$ is the observed variability of soil moisture and $\Delta\theta^{sim}$ is the simulated variability of soil moisture. Note that we consider $\Delta\theta$ for this optimization because of its relevance to the water flux and recharge through chalk unsaturated zone [e.g., *Ireson and Butler*, 2011]. Latin hypercube technique [e.g., *McKay et al.*, 2016] is used to generate 2000 random samples for each BC model parameter within the respective range discussed above.

We perform simulations using these random samples and calculate model performance (Equation 2) to select the optimum parameter values for the BC model (discussed in section 4.1).

3. Methods

3.1. Study area

The study area encompasses the Kennet catchment located in the Southern England with an area of about 1033 km^2 (Figure 1a). Generally, Kennet is rural in nature with scattered settlements and has a maximum altitude of approximately 297 m (Above Ordnance Level). The River Kennet discharges into the North Sea through London. The major tributaries of this river are Lambourn, Dun, Enborne, and Foudry Brook. An average annual rainfall of approximately 760 mm was recorded in the catchment over a 40 year period from 1961-1990.

Solid geology of the Kennet catchment is dominated by chalk, which is overlain by thin soil layer. While lower chalk outcrops along the northern catchment boundary, progressively younger rocks are found in the southern part. In general, surface runoff production is very limited over the regions of the catchment where chalk outcrops. The flow regime shows a distinct characteristics of slow response to groundwater held within the chalk aquifer [*Le Vine et al.*, 2016]. According to *Ireson and Butler* [2013], the unsaturated zone of chalk shows slow drainage over summer and bypass flow during wet periods in this catchment.

3.2. Field measurements and remotely sensed data

Table 1 summarizes the field measurements and remote sensing data used in this study. We use *in-situ* soil moisture and runoff measurements along with remotely sensed LE data to assess model performance in simulating the mass and energy balance components of the hydrological cycle. Point scale soil moisture measurements at two adjacent sites (~20 m apart) at the Warren Farm (Figure 1) were provided by Centre for Ecology and Hydrology

(CEH). A Didcot neutron probe was used at these locations to measure fortnightly soil moisture at different depths below land surface (10 cm apart down to 0.8 m, 20 cm apart between 0.8-2.2 m, and 30 cm apart between 2.2-4.0 m) [*Hewitt et al.*, 2010].

The National River Flow Archive (NRFA) coordinates discharge measurements from the gauging station networks across UK. These networks are operated by the Environmental Agency (England), Natural Resources Wales, Scottish Environment Protection Agency, and Rivers Agency (Northern Ireland). We use discharge measurement provided by NRFA to calculate the runoff ratio over the Kennet catchment in this study.

The MOD16 product of the Moderate Resolution Imaging Spectroradiometer (MODIS) is a part of NASA/EOS project that provides estimation of global terrestrial LE. The LE estimation from MOD16 is based on remotely sensed land surface data [e.g., *Mu et al.*, 2007]. In this study, the 8-day and monthly LE data products from MODIS is used to evaluate the model performance in simulating land surface energy fluxes.

3.3. Land surface model

In this study, we use the Joint UK Land Environment Simulator (JULES [e.g., *Best et al.*, 2011; *Clark et al.*, 2011]) version 4.2. JULES is a flexible modelling platform with a modular structure aligned to various physical processes developed based on the Met Office Surface Exchange Scheme (MOSES [e.g., *Cox et al.*, 1999; *Essery et al.*, 2003]). Meteorological data including precipitation, incoming short- and longwave radiation, temperature, specific humidity, surface pressure, and wind speed are required to drive JULES. Each grid box in JULES can comprise nine surface types (broadleaf trees, needle leaf trees, C3 grass, C4 grass, shrubs, inland water, bare soil, and ice) represented by respective fractional coverage. Each surface type is represented by a tile and a separate energy balance is calculated for each tile.

Subsurface heat and water transport equations are solved based on finite difference approximation in JULES as described in *Cox et al.* [1999]. Moisture transport in the subsurface is described by the finite difference form of Richards' equation. The vertical soil moisture flux is calculated using the Darcy's law. While the top boundary condition to solve the Richards' equation is infiltration at soil surface, the bottom boundary condition in JULES is free drainage that contributes to subsurface runoff.

Surface runoff is calculated by combining the equations of throughfall and grid box average infiltration in JULES. In order to direct the generated runoff to a channel network, river routing is implemented based on the discrete approximation of one-dimensional kinematic wave equation [e.g., *Bell et al.*, 2007]. In this approach, river network is derived from the digital elevation model (DEM) of the study area and different wave speeds are applied to surface and subsurface runoff components and channel flows [e.g., *Bell and Moore*, 1998]. A return flow term accounts for the transfer of water between subsurface and land surface [e.g., *Dadson et al.*, 2010, 2011].

3.4. Model configurations and input data

In this study, simulations are performed at two distinct spatial scales, namely point and catchment. At the point scale, JULES is configured to simulate the mass and energy fluxes at the Warren Farm site (Figure 1a). A total subsurface depth of 5 m is considered in the model with a vertical discretization ranging from 10 cm at the land surface to 50 cm at the bottom of the model domain. Note that this discretization is consistent with the soil moisture measurement depths mentioned in section 3.2. The vegetation type is implemented as C3 grass using the default parameters in JULES. Point scale simulations were performed over 2 consecutive years from 2003-2005 at an hourly time step. Except for precipitation, hourly atmospheric forcing data to drive JULES was obtained from an automatic weather station operated by the CEH at Warren Farm. In order to estimate hourly precipitation data to run JULES, rain gauge measurements from the Met Office [*Met Office*, 2006] were used. Inverse distance interpolation technique [e.g. *Garcia et al.*, 2008; *Ly et al.*, 2013] was applied on rainfall measurements from 13 gauges closest to Warren Farm (distance varies from 25-60 km) to obtain hourly precipitation for the point scale simulations.

At the catchment scale, JULES is configured over a study area encompassing the Kennet catchment (Figure 1a) considering a uniform lateral grid resolution of 1 km with 70 x 40 cells in x and y dimensions, respectively. The total subsurface depth and vertical discretization are identical to those of the point scale simulations. Spatially distributed vegetation type information for the study area (Figure 1b) is obtained from the Land Cover Map 2007 (LCM2007) dataset [*Morton et al.*, 2011]. Simulations were performed over 5 consecutive years from 2006-2011 at the catchment scale. Note that the simulation periods of catchment and point scale (2003-2005) does not coincide due to the availability of soil moisture measurements described in section 3.2. Spatially distributed meteorological data from the Climate, Hydrology and Ecology research Support System (CHESS) was used to obtain the atmospheric forcing to drive JULES at the catchment scale. The CHESS data includes 1 km resolution gridded daily meteorological variables [*Robinson et al.*, 2015]. This daily data is downscaled using a disaggregation technique described in *Williams and Clark* [2014] to obtain hourly atmospheric forcing. The flow direction required for river routing is extracted from the USGS HydroSHEDS digital elevation data [*Lehner et al.*, 2008].

We estimate the soil hydraulic properties based on texture (Table 2). At the point scale, loam soil is dominant at the Warren Farm site. At the catchment scale, the Harmonized World Soil Database (HWSD) from the Food and Agricultural Organization of UNO (FAO) is used to obtain the texture of different soil types over Kennet (Figure 1c). The saturation-pressure head relationship for different soil types is described using the Van Genuchten [*Van*

Genuchten, 1980] model with parameter values (Table 2) obtained from *Schaap and Leij* [1998].

Table 3 summarizes the hydraulic properties for chalk used in this study. These properties are obtained based on existing literature as a first step when evaluating the uncalibrated BC model. The BC model parameters are subsequently optimized to minimize the differences between observed and simulated $\Delta\theta$.

In this study, we consider two different model configurations, namely *default* and *macro* (Figure 2). The *default* configuration corresponds to the standard parameterizations of JULES that does not represent chalk hydrology in the model. In this configuration, each soil column in JULES is considered to be vertically homogeneous with the soil properties defined in Table 2, which is motivated by the Met Office JULES Global Land 4.0 configuration described in *Walters et al.* [2014]. The *macro* configuration, in contrast, explicitly represents chalk by applying the BC model starting at 30 cm below land surface to the bottom of the model domain (i.e. 500 cm). Therefore, the soil column in the *macro* configuration can be divided into topsoil (0-30 cm) and chalk (30-500 cm) in *macro*. Note that except for this inclusion of chalk, *default* and *macro* configurations are identical in terms of model set up and input data.

The topsoil depth of 30 cm in the *macro* configuration is defined based on several augured soil samples collected during a field campaign at Warren Farm in 2015 (Figure 2). This depth is corroborated by additional information from the British Geological Survey (BGS) operated borehole records (http://www.ukso.org/pmm/soil_depth_samples_points.html), which show that topsoil depths vary from 10-40 cm over the study area. We therefore apply the *macro* configuration assuming a spatially homogeneous topsoil depth of 30 cm for both point and catchment scale simulations.

4. Results and discussion

4.1. Point scale simulations

At the point scale, the simulation results are evaluated using soil moisture observations at the Warren Farm site. Figure 3a compares observed and simulated soil moisture (θ) from the *default* and *macro* configurations at 2 m below land surface. Note that the *macro* configuration uses the chalk hydraulic parameters collected from existing literature (Table 3). This figure shows that the *default* configuration underestimates θ throughout the simulation period, which is improved remarkably in case of *macro*. Figure 3b plots observed and simulated soil moisture variability ($\Delta\theta$) from the *default* and *macro* configurations at the Warren Farm site. In general, both configurations show discrepancies with observed $\Delta\theta$ with *macro* showing relatively better model performance.

The results show that despite the *macro* configuration improves simulated θ, it shows considerable discrepancies with observed $\Delta\theta$, which is consistent throughout the whole chalk profile (results from other model layers are not shown). In order to minimize the differences between observed and modelled $\Delta\theta$ from the *macro* configuration, we optimize the BC model following the methodology described in section 2. The optimization results are summarized in Figure 4. Note that for each combination considered in the optimization, 2000 model runs were performed using randomly sampled parameters as discussed in section 2. Figure 4 presents the results from the model runs yielding the lowest RMSE.

The RMSE between observed and simulated $\Delta\theta$ for the model configurations considered in the optimization is shown in Figure 4a. This figure illustrates that the RMSE of the *default* configuration is larger than that of *macro*, indicating better model performance in reproducing $\Delta\theta$ for the latter. Therefore, it appears that the uncalibrated BC model (i.e., the *macro* configuration) is better in reproducing soil moisture variability compared to *default*.

Figure 4b, c and d presents the BC model parameter values from the model run producing the lowest RMSE for each configuration. Concerning single BC model parameters, Figure 4a shows that optimizing S_0 results in a 16% reduction of RMSE compared to the *macro* configuration. Optimizing K_s marginally improves model performance, which is observed from a slightly lower (4%) RMSE than *macro*. Optimizing both K_s and S_0 simultaneously results in the largest reduction (24%) of RMSE compared to *macro*.

Additionally, Figure 4 suggests that the sensitivity of S_0 on the model performance in simulating $\Delta\theta$ is substantially higher compared to K_s and f_m, which is corroborated by the sensitivity of the individual model parameters (Figure S2). Figure 4a also reveals the interesting fact that the RMSE from the configuration with optimized K_s and S_0 is identical to that of the one with all 3 parameters optimized simultaneously (i.e., K_s, S_0 and f_m). Therefore, we select the *macro* configuration with optimized K_s and S_0 ($macro_{opt}$ hereafter) to simulate chalk hydrology over the study area.

Figure 5 compares $\Delta\theta$ from the $macro_{opt}$ configuration ($\Delta\theta_{opt}$) with observed soil moisture variability ($\Delta\theta_{obs}$). As mentioned earlier, $\Delta\theta_{default}$ and $\Delta\theta_{macro}$ show considerable discrepancies with $\Delta\theta_{obs}$ while the *macro* configuration exhibits relatively better performance. Figure 5 illustrates that the overall agreement between observed and simulated $\Delta\theta$ improves substantially in case of $macro_{opt}$ compared to *default* and *macro,* which is pronounced especially in the deeper chalk layers. Therefore, this figure indicates that the performance of the BC model in simulating $\Delta\theta$ is further improved by optimizing the K_s and S_0 parameters at the Warren Farm site.

In order to assess the model performance in simulating soil moisture over the entire column, the relative bias ($\Delta\mu$, see Appendix) of simulated θ from the *default* and $macro_{opt}$ configurations at Warren Farm for various depth ranges are shown in Figure 6. In the soil layers (0-30 cm), θ from the two configurations are comparable with the *default* showing slightly lower mean relative bias ($\Delta\mu_{mean}$) of -0.03 than *macro*$_{opt}$ ($\Delta\mu_{mean}$ = -0.09). However, in the chalk layers (30-500 cm), *default* simulates substantially drier conditions, corresponding to $\Delta\mu_{mean} \leq -0.28$. In contrast, the *macro*$_{opt}$ configuration considerably improves the agreement between the simulated and observed θ in the chalk layers with $\Delta\mu_{mean} \geq -0.05$. Therefore, the results indicate that the inclusion of the BC model in JULES improves the performance of overall soil moisture simulation (both θ and $\Delta\theta$) at Warren Farm especially in the chalk layers.

The drainage flux through the bottom of soil column (d_b) of a land surface model can be considered as the potential recharge flux to groundwater [e.g., *Sorensen et al.*, 2014]. Figure 7 compares the daily sum of d_b from the *default* and *macro*$_{opt}$ configurations at the Warren Farm site. The rainfall characteristics over the study period is shown in Figure 7a. In Figure 7b, the *macro*$_{opt}$ configuration shows considerable d_b during the colder months, while slow drainage prevails throughout the rest of the year. In contrast, the *default* configuration shows relatively high d_b in summer compared to the colder months. In general, the recharge rate through chalk unsaturated zone during the warmer periods of the year is lower than that in the winter months [*Wellings and Bell*, 1980; *Ireson et al.*, 2009]. Therefore, the *macro*$_{opt}$ configuration appears to be more consistent with the recharge mechanism in chalk compared to *default*.

In this section, the BC model was evaluated at the point scale. The results showed that in general, the *macro* configuration performs relatively better in simulating θ and $\Delta\theta$ compared to *default*. In order to improve the model performance even further, parameter optimization was performed to minimize the differences between observed and simulated $\Delta\theta$ at the point scale. In the next sections, the optimized model (*macro*$_{opt}$) is evaluated at the catchment scale.

4.2. Catchment scale simulations

In the previous section, it was observed that the *default* configuration generally underestimates θ compared to $macro_{opt}$. Previous studies have demonstrated the interconnections between shallow soil moisture and LE [e.g., *Chen and Hu*, 2004]. In order to assess the differences between the LE from the *default* and $macro_{opt}$ configurations at the catchment scale, Figure 8 plots spatially averaged 8-day composites of LE from MODIS (LE_{MOD}) against the LE from these configurations ($LE_{default}$ and LE_{opt}, respectively) over Kennet. The agreement between simulated LE and LE_{MOD} is evaluated using the coefficient of determination (R^2, see Appendix) and mean bias. Comparison between $LE_{default}$ and LE_{MOD} shows a coefficient of determination of $R^2_{default}$ = 0.78 and a mean bias of $bias_{default}$ = 10.5 Wm^{-2}. The agreement between simulated LE and LE_{MOD} improves in case of the $macro_{opt}$ configuration, which is reflected by an increased coefficient of determination of R^2_{opt} = 0.81 and a reduced mean bias of $bias_{opt}$ = 3 Wm^{-2}.

Figure 8 shows differences between $LE_{default}$ and LE_{opt} especially for relatively high *LE*, indicating discrepancies especially during the warmer months of the year. Figure 9 presents spatially averaged time series of monthly LE_{MOD}, $LE_{default}$ and LE_{opt}. This figure shows that the differences between $LE_{default}$ and LE_{opt} increases substantially in summer compared to the colder months of the year, which is consistent with Figure 8. Consequently, the *default* configuration underestimates *LE* in summer compared to LE_{MOD}, which is improved in case of the $macro_{opt}$ configuration. In contrast, the differences between $LE_{default}$ and LE_{opt} are negligible during the colder months of the year.

Table 4 compares observed and simulated daily average runoff from the two model configurations over the Kennet catchment from 2006-2011. The runoff ratio (*RR*, see Appendix), which is equal to the mean volume of flow divided by the volume of precipitation [e.g., *Kelleher et al.*, 2015], assesses the partitioning of precipitation into runoff over the catchment. The *default* configuration (*RR* = 0.82) shows considerably higher *RR* compared to observation (*RR* = 0.40), indicating overestimation of runoff by the model. Including chalk hydrology in the model remarkably improves the agreement between observed and simulated mean runoff over the Kennet catchment, which is assessed from a runoff ratio of *RR* = 0.37 for the $macro_{opt}$ configuration.

In Table 4, the relative bias (Δμ) of 1.04 between observed and simulated runoff from the *default* configuration again indicates the overestimation by the model. In comparison, $macro_{opt}$ shows a relative bias (Δμ =-0.05), indicating improvement between observed and simulated mean runoff volume compared to *default*. The relative difference in standard deviation (Δσ, see Appendix) compares the variability of observed and simulated runoff in Table 4. This comparison shows that the *default* configuration overestimates the variability of runoff over the Kennet catchment (Δσ = 2.04), which is improved in case of *macro* (Δσ = 0.70).

It was demonstrated previously that the *default* configuration predicts lower evapotranspiration (ET) compared to $macro_{opt}$ over the Kennet catchment due to the differences in simulated θ. In JULES, moisture from soil and canopy is depleted to meet the ET demand. Additionally, surface runoff generation depends on canopy water storage in the model [*Best et al.*, 2011]. Because of this connection between ET and surface runoff generation via canopy water storage, the differences in runoff demonstrated in Table 4 can be attributed to the disagreements between $LE_{default}$ and LE_{macro} (Figure 8) due to the relatively drier conditions simulated by *default*.

In this section, the BC model is evaluated using observed mass and energy fluxes over the Kennet catchment. The *default* configuration showed considerably low LE over the catchment, which was pronounced during the warmer period of the year. The agreement between observed and simulated LE was improved in case of the $macro_{opt}$ configuration compared to *default*. It was also observed that the overall runoff prediction was improved by $macro_{opt}$ compared to *default*. Given its simplicity, our results indicate that the proposed parameterization is suitable for use in land surface modelling applications.

5. Summary and Conclusions

In this study, we proposed a simple parameterization, namely the *Bulk Conductivity* (BC) model to simulate water flow through the matrix-fracture system of chalk in large scale land surface modelling applications. This parameterization was implemented in the Joint UK Land Environment Simulator (JULES) and applied to the Kennet catchment located in the southern UK to simulate the mass and energy fluxes of the hydrological cycle for multiple years. Two model configurations, namely *default* and *macro* were considered with the latter using the BC model to simulate chalk hydrology.

The proposed BC model is a single continuum approach of modelling preferential flow [e.g., *Beven and Germann*, 2013] that involves only 2 parameters, namely macroporosity factor (f_m) and relative saturation threshold (S_0). Initially, these parameters along with the saturated hydraulic conductivity of the chalk matrix were estimated from existing literature. Finally, the BC model parameters were optimized to minimize the differences between observed and simulated soil moisture variability. Our results indicated that S_0 is the most influential parameter in the model when representing water movement through a soil-chalk column, followed by the saturated hydraulic conductivity of chalk matrix while f_m showed low sensitivity. Hence, the parameterization is further improved by optimizing both saturated hydraulic conductivity of chalk matrix and S_0 to minimize the differences between observed and simulated soil moisture variability.

The simulation results were evaluated using observed mass and energy fluxes both at point and catchment scales. The results demonstrated that the inclusion of the BC model in JULES improves simulated soil moisture variability at the point scale compared to a model configuration that does not represent chalk in the subsurface (i.e., the *default* configuration). At the catchment scale, it was illustrated that the proposed parameterization improves simulated latent heat flux and overall runoff compared to the *default* configuration.

Note that the complexity of the BC model for simulating water flow through chalk unsaturated zone is substantially lower compared to more commonly used models for this purpose (e.g., dual-porosity models). Despite its simplicity, it appears that the proposed parameterization improves mass and energy fluxes simulated by JULES over the Kennet catchment. As mentioned previously, representing chalk hydrology in land surface models using the dual-porosity concept is complicated mainly due to the relatively large number of parameters involved in such approach. Therefore, the simplified parameterization proposed in this study may be useful for large-scale land surface modelling applications over chalk-dominated areas.

Acknowledgements

We gratefully acknowledge the support by the “A MUlti-scale Soil moisture Evapotranspiration Dynamics study – AMUSED” project funded by Natural Environment Research Council (NERC) grant number NE/M003086/1. The authors would also like to thank Ned Hewitt and Jonathan Evans from the Centre for Ecology and Hydrology (CEH) for providing the data for the point-scale analyses at the Warren Farm. Finally, we would like to thank Miguel Rico-Ramirez (University of Bristol) for helping preparing the precipitation data from the rain gauge network used for the point-scale simulations, Thorsten Wagener (University of Bristol) for his valuable suggestions on model diagnostics, and Joost Iwema

(University of Bristol) for helping with the soil samples collected during the 2015 field work campaign.

Appendix

Definition of Statistical Metrics

Coefficient of determination (R^2) for observation y = y1, …, yn and prediction f = f1, …, fn is defined as

$$R^2 = 1 - \frac{SS_{res}}{SS_{tot}}$$

where, SS_{res} is the residual sum of square and SS_{tot} is the total sum of square. SS_{res} and SS_{tot} are defined as

$$SS_{res} = \sum_{i=1}^{n}(y_i - f_i)^2 \quad \text{and}$$

$$SS_{tot} = \sum_{i=1}^{n}(y_i - \bar{y})^2 \quad \text{with } \bar{y} \text{ being the mean of y.}$$

Runoff ratio (RR) assesses the portion of precipitation that generates runoff over the catchment. RR is defined as

$$RR = \frac{\mu_{runoff}}{\mu_{rain}}$$

where μ_{runoff} is mean runoff and μ_{rain} is mean precipitation [e.g., *Kelleher et al.*, 2015].

Relative bias ($\Delta\mu$) between observed and simulated time series can be defined as

$$\Delta\mu = \frac{\mu_{mod} - \mu_{obs}}{\mu_{obs}}$$

where μ_{obs} and μ_{mod} are the mean of observed and simulated time series, respectively. While the optimal value of $\Delta\mu$ is zero, negative (positive) values indicate an underestimation (overestimation) by the model [e.g., *Gudmundsson et al.*, 2012].

Relative difference in standard deviation ($\Delta\sigma$) between observed and simulated time series can be defined as

$$\Delta\sigma = \frac{\sigma_{mod} - \sigma_{obs}}{\sigma_{obs}}$$

where σ_{obs} and σ_{mod} are the standard deviation of observed and simulated time series, respectively [e.g., *Gudmundsson et al.*, 2012].

References

Bakopoulou, C. (2015), Critical assessment of structure and parameterization of JULES land surface model at different spatial scales in a UK Chalk catchment, PhD thesis, Imperial College London, UK, available at: https://spiral.imperial.ac.uk:8443/handle/10044/1/28955.

Bell, V. A. and R. J. Moore (1998), A grid-based flood forecasting model for use with weather radar data: Part 1. Formulation, Hydrol. Earth Syst. Sc., 2, 265-281.

Bell, V. A., A. L. Key, R. G. Jones, and R. J. Moore (2007), Development of a high resolution grid-based river flow model for use with regional climate model output, Hydrol. Earth Syst. Sc., 11, 532-549.

Best, M. J., M. Pryor, D. B. Clark, G. G. Rooney, R. l. H. Essery, C. B. Ménard, J. M. Edwards, M. A. Hendry, A. Porson, N. Gedney, L. M. Mercado, S. Sitch, E. Blyth, O. Boucher, P. M. Cox, C. S. B. Grimmond, and R. J. Harding (2011), The Joint UK Land Environment Simulator (JULES), Model Description – Part 1: Energy and Water Fluxes, Geosci. Model Dev., 4, 677-699.

Beven, K., and P. Germann (2013), Macropores and water flow in soils revisited, Water Resour. Res., 49, 3071‑3092.

Bloomfield, J. (1997), The role of diagenesis in the hydrogeological stratification of carbonated aquifers: An example from the chalk at Fair Cross, Berkshire, UK, Hydrol. Earth Syst. Sc., 1, 19-33.

Blume, T. (2008), Hydrological processes in volcanic ash soils: measuring, modelling and understanding runoff generation in an undisturbed catchment, PhD thesis, Institut für

Geoökologie, Universität Potsdam, Potsdam, Germany, available at: https://publishup.uni-potsdam.de/opus4-ubp/files/1524/blume_diss.pdf

Brouyère, S. (2006), Modelling the migration of contaminants through variably saturated dual-porosity, dual-permeability chalk, J. Contam, Hydrol., 82, 195-219.

Chen, X., and Q. Hu (2004), Groundwater influences on soil moisture and surface evaporation, J. Hydrol., 297, 285–300.

Clark, D. B., L. M. Mercado, S. Sitch, C. D. Jones, N. Gedney, M. J. Best, M. Pryor, G. G. Rooney, R. L. H. Essery, E. Blyth, O. Boucher, R. J. Harding, C. Huntingford, and P. M. Cox (2011), The Joint UK Land Environment Simulator (JULES), Model Description – Part 2: Carbon Fluxes and Vegetation Dynamics, Geosci. Model Dev. 4, 701-722.

Cox, P. M., R. A. Betts, C. B. Bunton, R. L. H. Essery, P. R. Rowntree and J. Smith (1999), The impact of new land surface physics on the GCM simulation of climate and climate sensitivity, Clim. Dynam., 15, 183-203.

Dadson, S. J., I. Ashpole, P. Harris, H. N. Davies, D. B. Clark, E. Blyth, and C. M. Taylor (2010), Wetland inundation dynamics in a model of land surface climate: Evaluation in the Niger inland delta region, J. Geophys. Res., 115.

Dadson, S. J., V. A. Bell, and R. G. Jones (2011), Evaluation of a grid based river flow model configured for use in a regional climate model, J. Hydrol., 411, 238-250.

Dettinger, M. D., and H. F. Diaz (2000), Global characteristics of streamflow seasonality and variability, J. Hydrometeorol., 1, 289-310.

Essery, R., M. Best, and P. Cox (2001), MOSES 2.2 technical documentation (Hadley Centre technical note 30), Hadley Centre, Met Office, UK.

Garcia, M., C. D. Peters-Lidard, and D. C. Goodrich (2008), Spatial interpolation of precipitation in a dense gauge network for monsoon storm events in the southwestern United States, Water Resour. Res., 44.

Gascoin, S., A. Duchare, P. Ribstein, M. Carli, and F. Habtes (2000), Adaptation of a catchment-based land surface model to the hydrological setting of the Somme River basin (France), J. Hydrol., 368, 105-116.

Gudmundsson, L., T. Wagener, L. M. Tallaksen, and K. Engeland (2012), Evaluation of nine large-scale hydrological models with respect to the seasonal runoff climatology in Europe, Water Resour. Res., 48.

Gupta, H. V., H. Kling, K. K. Yilmaz, and G. F. Martinez (2009), Decomposition of the mean squared error and NSE performance criteria: implications for improving hydrological modelling, J. Hydrol., 377, 80-91.

Haria, A. H., M. G. Hodnett, and A. C. Johnson (2003), Mechanisms of groundwater recharge and pesticide penetration to chalk aquifer in southern England, J. Hydrol., 275, 122-137.

Hartmann, A., N. Goldscheider, T. Wagener, J. Lange, and M. Weiler (2014), Karst water resources in a changing world: Review of hydrological modeling approaches, Rev. Geophys., 52, 218–242, doi:10.1002/2013RG000443.

Hewitt, N., M. Robinson, and D. McNeil (2010), Pang and Lambourn hydrometric review 2009, Wallingford, NERC/Centre for Ecology and Hydrology, (CEH project number: C04076).

Ireson, A. M., S. A. Mathias, H. S. Wheater, A. P. Butler and J. Finch (2009), A model for flow in the chalk unsaturated zone incorporating progressive weathering, J. Hydrol., 365, 244-260.

Ireson, A. M. and A. P. Butler (2011), Controls on preferential recharge to chalk aquifers, J. Hydrol., 398, 109-123.

Ireson, A. M. and A. P. Butler (2013), A critical assessment of simple recharge models: application to the UK chalk, Hydrol. Earth Syst. Sc., 17, 2083-2096.

Ireson, A. M., H. S. Wheater, A. P. Butler, S. A. Mathias, J. Finch, and J. D. Cooper (2006), Hydrological processes in the chalk unsaturated zone – insight from an intensive field monitoring program, J. Hydrol., 330, 29-43.

Ireson, A. M., S. A. Mathias, H. S. Wheater, A. P. Butler, and J. Finch (2009), A model for flow in the chalk unsaturated zone incorporating progressive weathering, J. Hydrol., 365, 244-260.

Jackson, C. and Spink, A. (2004) User's Manual for the Groundwater Flow Model ZOOMQ3D, IR/04/140, British Geological Survey, Nottingham, UK.

Kelleher, C., T. Wagener, and B. McGlynn (2015), Model-based analysis of the influence of catchment properties on hydrologic partitioning across five mountain headwater subcatchments, Water Resour. Res., 51, 4109-4136.

Kling, H., M. Fuchs, and M. Paulin (2012), Runoff conditions in the upper Danube basin under an ensemble of climate change scenarios. Journal of Hydrology, Volumes 424-425, 6 March 2012, 264-277.

Lehner, B., K. Verdin, and A. Jarvis (2008), New global hydrography derives from spaceborne elevation data, EOS, Transactions, AGU, 89(10), 93-94.

Le Vine, N., A . Butler, N. McIntyre, and C. Jackson (2016), Diagnosing hydrological limitations of a land surface model: application of JULES to a deep-groundwater chalk basin, Hydrol. Earth Syst. Sc., 20, 143-159.

Lee, L. J. E., D. S. L. Lawrence, and M. Price (2006), Analysis of water-level response to rainfall and implications for recharge pathways in the chalk aquifer, SE England, J. Hydrol., 330, 604-620.

Ly, S., C. Charles, and A. Degré (2013), Different methods for spatial interpolation of rainfall data for operational hydrology and hydrological modeling at watershed scale. A review, Biotechnol. Agron. Soc. Environ. 17, 392-406.

Mathias, S. A., A. P. Butler, B. M. Jackson, and H. S. Wheater (2006), Transient simulations of flow and transport in the chalk unsaturated zone, J. Hydrol., 330, 10-28.

Met Office (2006), UK hourly rainfall data, Part of the Met Office Integrated Data Archive System (MIDAS), NCAS British Atmospheric Data Centre, 21 March 2016, http://catalogue.ceda.ac.uk/uuid/bbd6916225e7475514e17fdbf11141c1.

Morton, D., C. Rowland, C. wood, L. Meek, C. Marston, G. Smith, R. Wadsworth, and I. C. Simpson (2011), Final report for LCM2007 – the new UK Land Cover Map (CS technical report no 11/07), Centre for Ecology and Hydrology, UK.

Mu, Q., F. A. Heinsch, M. Zhao, and S. W. Running (2007), Development of a global evapotranspiration algorithm based on MODIS and global meteorology data, Remote Sens. Environ., 111, 519-536.

Price, A., R. A. Downing, and W.M. Edmunds (1993), The chalk as an aquifer. In: Downing, R. A., M. Price, and G. P. Jones *The hydrogeology of the chalk of north-west Europe*. Oxford: Claredon Press. 35-58.

Price, M., R. G. Low, and C. McCann (2000), Mechanisms of water storage and flow in the unsaturated zone of chalk aquifer, J. Hydrol., 54-71.

Rawls, W. J., D. L. Brankensiek, and K. E. Saxton (1982), Estimation of soil water properties, Trans. ASAE, 25(5), 1316–1320.

Robinson, E. L., E. Blyth, D. B. Clark, J. Finch, and A. C. Rudd (2015), Climate hydrology and ecology research support system potential evapotranspiration dataset for Great Britain (1961- 2012) [CHESS-PE], NERC-Environmental Information Data Centre.

Schär C., D. Lüthi, U. Beyerle, and E. Heise (1999), A soil precipitation feedback: A process study with a regional climate model, J. Clim., 12, 722–741.

Schaap, M. G., and F. J. Leij (1998), Database-related accuracy and uncertainty of pedotransfer functions, Soil Sci., 163(10), 765‑779.

Sorensen, J. P. R., J. W. Finch, A. M. Ireson, and C. R. Jackson (2014), Comparison of varied complexity models simulating recharge at the field scale, Hydrol. Process., 28, 2091-2102.

Van den Daele, G. F. A., J. A. Barker, L. D. Connell, T. C. Atkinson, W. G. Darling, and J. D. Cooper (2007), J. Hydrol., 342, 157-172.

Van Genuchten, M. Th. (1980), A closed-form equation for predicting the hydraulic conductivity of unsaturated soils, Soil Sci. Soc. Am. J., 44, 892‑898.

Walters, D. N., K. D. Williams, I. A. Boutle, A. C. Bushell, J. M. Edwards, P. R. Field, A. P. Lock, C. J. Morcrette, R. A. Stratton, J. M. Wilkinson, M. R. Willett, N. Bellouin, A. Bodas-Salcedo, M. E. Brooks, D. Copsey, P. D. Earnshaw, S. C. Hardiman, C. M. Harris, R. C. Levine, C. MacLachlan, J. C. Manners, G. M. Martin, S. F. Milton, M. D. Palmer, M. J. Roberts, J. M. Rodríguez, W. J. Tennant, and P. L. Vidale (2014), The Met Office unified model global atmosphere 4.0 and JULES global land 4.0 configurations, Geosci. Model Dev., 7, 361-386.

Welliings, S. R., and J. P. Bell (1980), Movement of water and nitrate in the unsaturated zone of upper chalk near Winchester, Hants., England, J. Hydrol, 48, 119-136.

Williams, K., and D. Clark (2014), Disaggregation of daily data in JULES (Hadley Centre technical note 96), Hadley Centre, Met Office, UK.

Zehe, E. and G. Blöschl (2004), Predictability of hydrologic response at the plot and catchment scales: Role of initial conditions, Water Resour. Res, 40.

Zehe, E., T. Maurer, J. Ihringer, and E.Plate (2001), Modeling water flow and mass transport in a loess catchment, Phys. Chem. Earth (B), 26, 487-507.

Zehe, E., U. Ehret, T. Blume, A. Kleidon, U. Scherer, and M. Westhoff (2013), A thermodynamic approach to link self-organization, preferential flow and rainfall-runoff behaviour, Hydrol. Earth Syst. Sc., 17, 4297-4322.

Tables

Table 1. Field measurements and remote sensing data.

Data	Spatial scale	Temporal extent	Frequency	Source
Soil moisture	Point[a]	2003-2005	15 day	N. Hewitt (CEH)
Latent heat flux	Global	2006-2011	8 day, 1 month	MODIS
Discharge	Point[b]	2006-2011	1 day	NRFA

[a]Measured at Warren Farm.
[b]Locations are shown in Figure 1a.

Table 2. Hydraulic properties for different soil types (refer to Figure 1c). Saturated hydraulic conductivity (K_s) and porosity data are obtained from *Rawls et al.* [1982]. The Van Genuchten parameters are acquired from *Schaap and Leij* [1998].

Texture	K_s (ms^{-1})	Porosity (-)	α (m^{-1})	n (-)
Loam	$3.7x10^{-6}$	0.463	3.33	1.56
Silt loam	$2.0x10^{-6}$	0.50	1.2	1.39
Clay	$1.7x10^{-7}$	0.475	2.12	1.2

Table 3. Hydraulic properties of chalk

Properties	Unoptimized		Optimized value
	Value	Source	
K_s (md^{-1})	16	Le Vine et al., 2016	15
S_0 (-)	0.8	Observations	0.67
f_m (-)	$1x10^5$	Price et al., 1993	$6.1x10^5$
α (m^{-1})	3.0	Le Vine et al., 2016	-
n (-)	1.4	Le Vine et al., 2016	-

Table 4. Comparison between observed and simulated daily average runoff from the two configurations over the Kennet catchment.

Metric	Observed	Simulated (*default*)	Simulated (*macro*)
RR	0.40	0.82	0.37
Δμ	-	1.04	-0.05
Δσ	-	2.04	0.70

Figures

Figure 1. Location (a), vegetation cover (b), and soil texture (c) over the study area. The red line in (a) outlines the Kennet catchment boundary, while the river network is shown in blue. The black triangle in (a) shows the location of the discharge gauging station at the catchment outlet while the black square corresponds to Warren Farm location where point-scale simulations are carried out. The shaded area in (c) represents the location of chalk in the catchment.

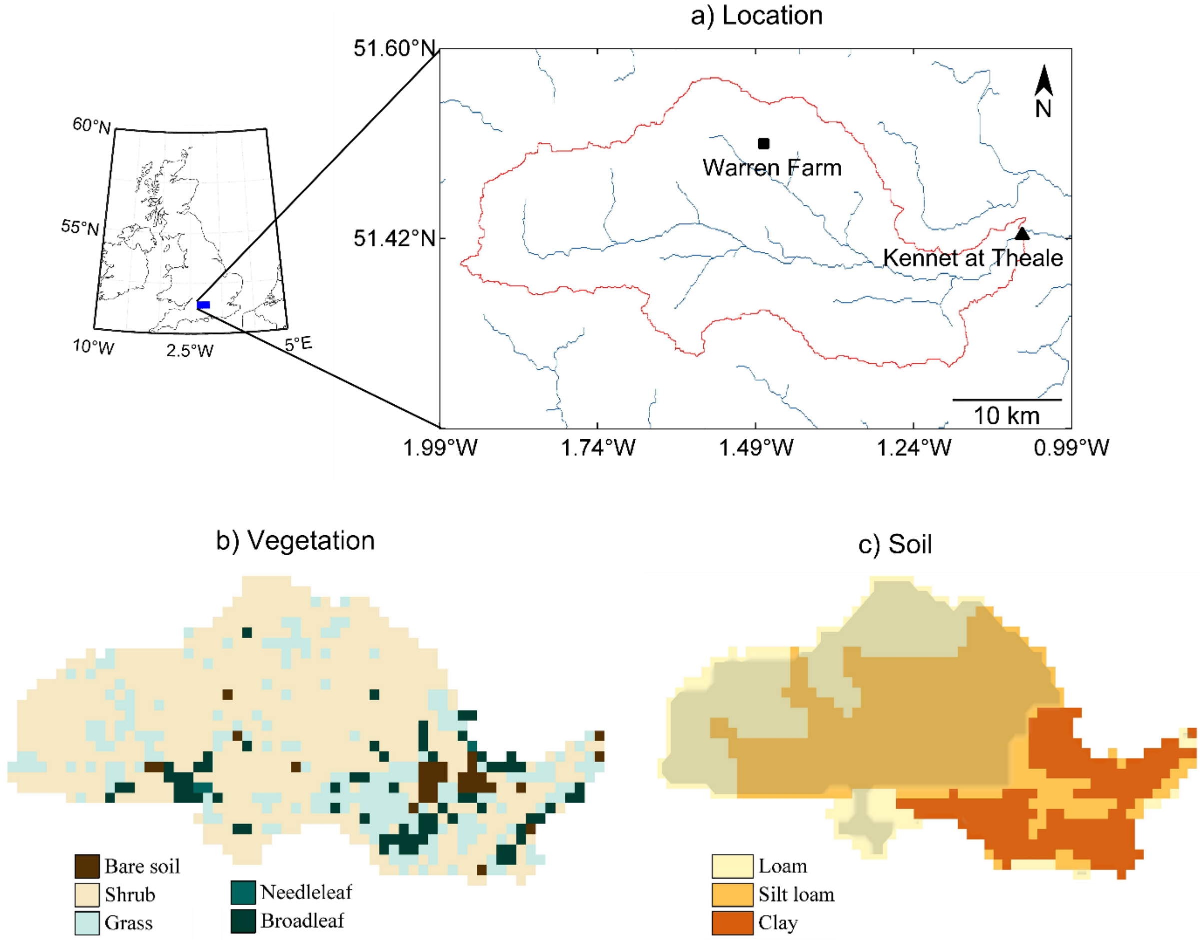

Figure 2. Example of soil profiles collected at Warren Farm during a field campaign in 2015 (a), and the two model configurations (b).

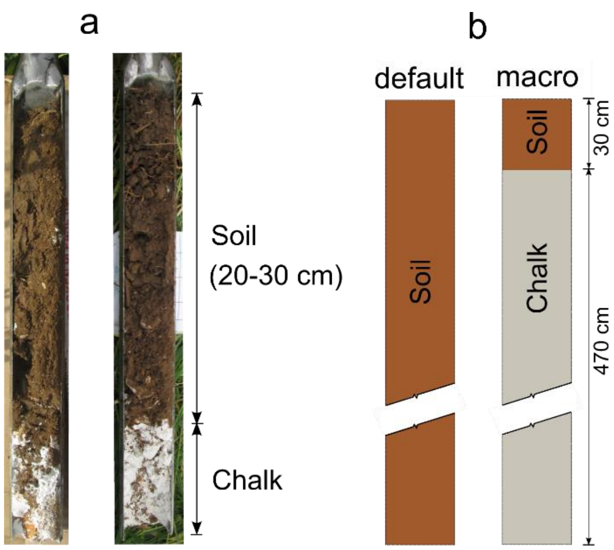

Figure 3. Comparison between observed and simulated (a) soil moisture (θ) and (b) change in soil moisture (Δθ) from the *default* and *macro* configurations at a depth of 2m below land surface. The shaded areas constructed from 2 soil moisture probes at the Warren Farm site denote the range of observed data in these plots.

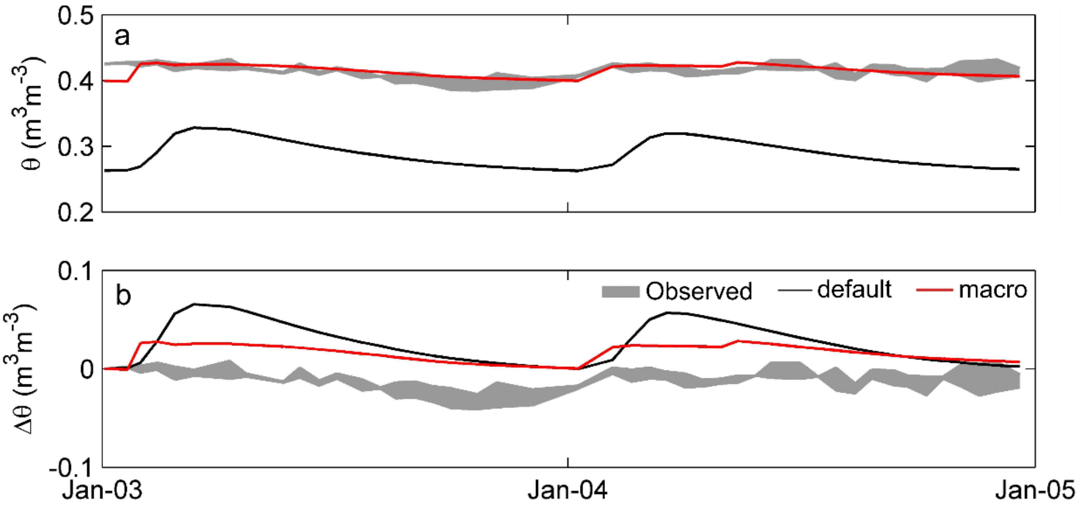

Figure 4. (a) Model performance in reproducing observed and simulated $\Delta\theta$, (b) K_s, (c) S_0 and (d) f_m for various parameter combinations considered in the optimization. Note that except for the *default* and *macro*, the simulation yielding the lowest RMSE (out of 2000 model runs) is presented in this plot.

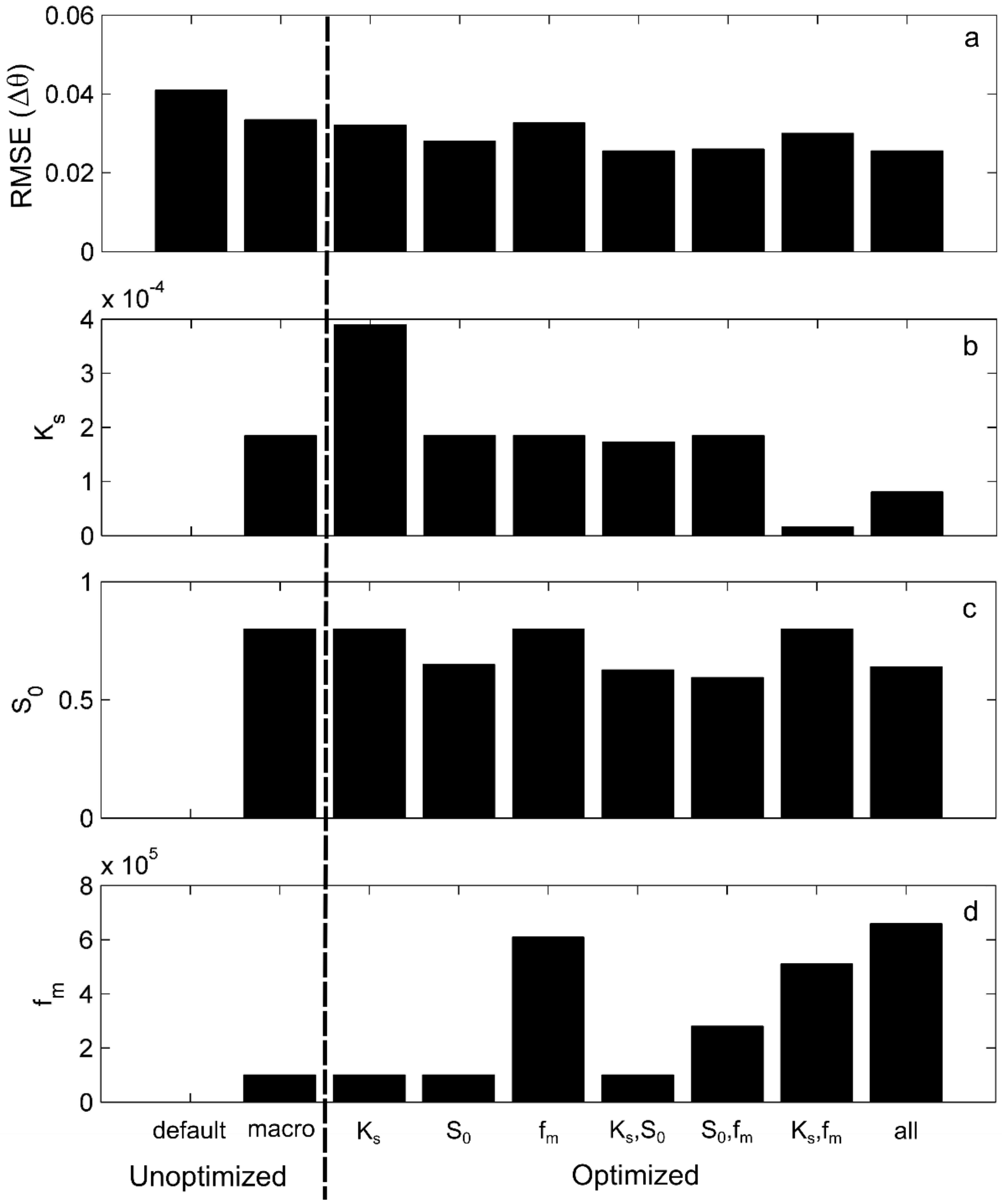

Figure 5. Comparison between observed and simulated $\Delta\theta$ from *default*, *macro* and $macro_{opt}$ configurations at various depths below land surface. The shaded area, which is constructed from 2 soil moisture probes at the Warren Farm site, denotes the range of $\Delta\theta$.

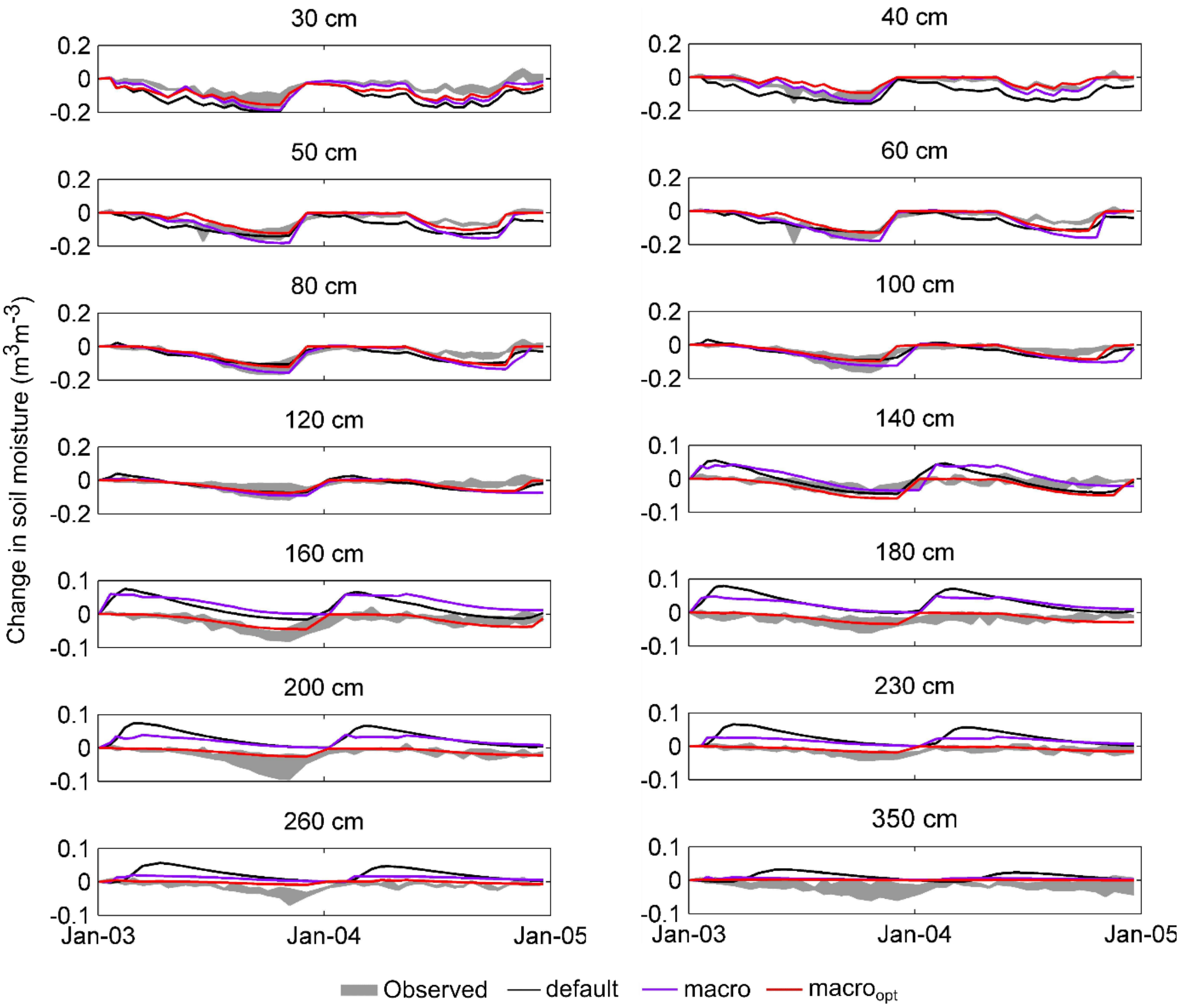

Figure 6. Box plot of relative bias (Δμ) of simulated soil moisture from *default* and *macro* configurations at different depth ranges shown in individual intervals (e.g., 0-30 cm, 30-100 cm, and so on).

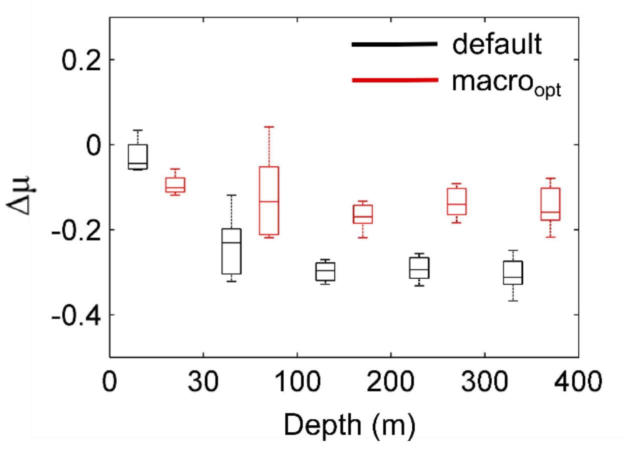

Figure 7. (a) Precipitation and (b) daily sum of drainage through the bottom of the soil column at Warren Farm over the two simulated years (2003-2005).

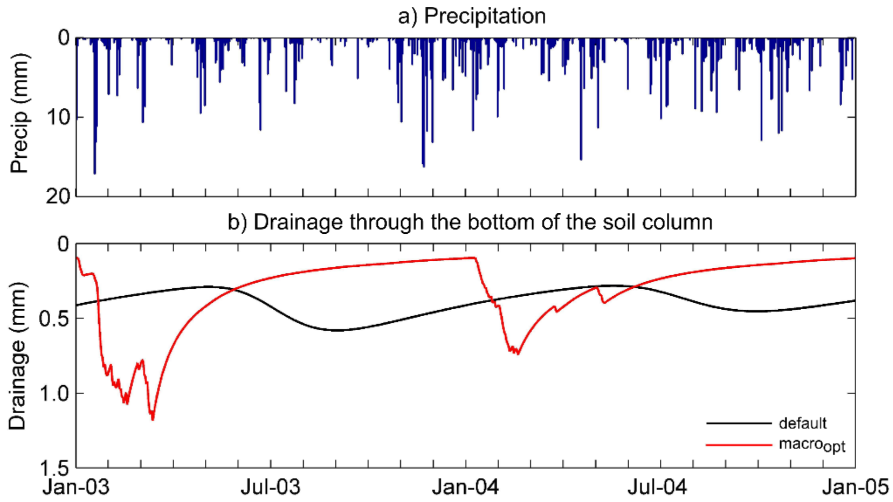

Figure 8. Catchment average 8 day composites of MODIS estimated *LE* (LE_{MOD}) against simulated *LE* from *default* and *macro* configurations ($LE_{default}$ and LE_{macro}, respectively) along with the linear models fitted for $LE_{default}$ (black line) and LE_{macro} (red line). The 1:1 line is shown in grey, which represents the perfect fit between LE_{MOD} and simulated *LE*.

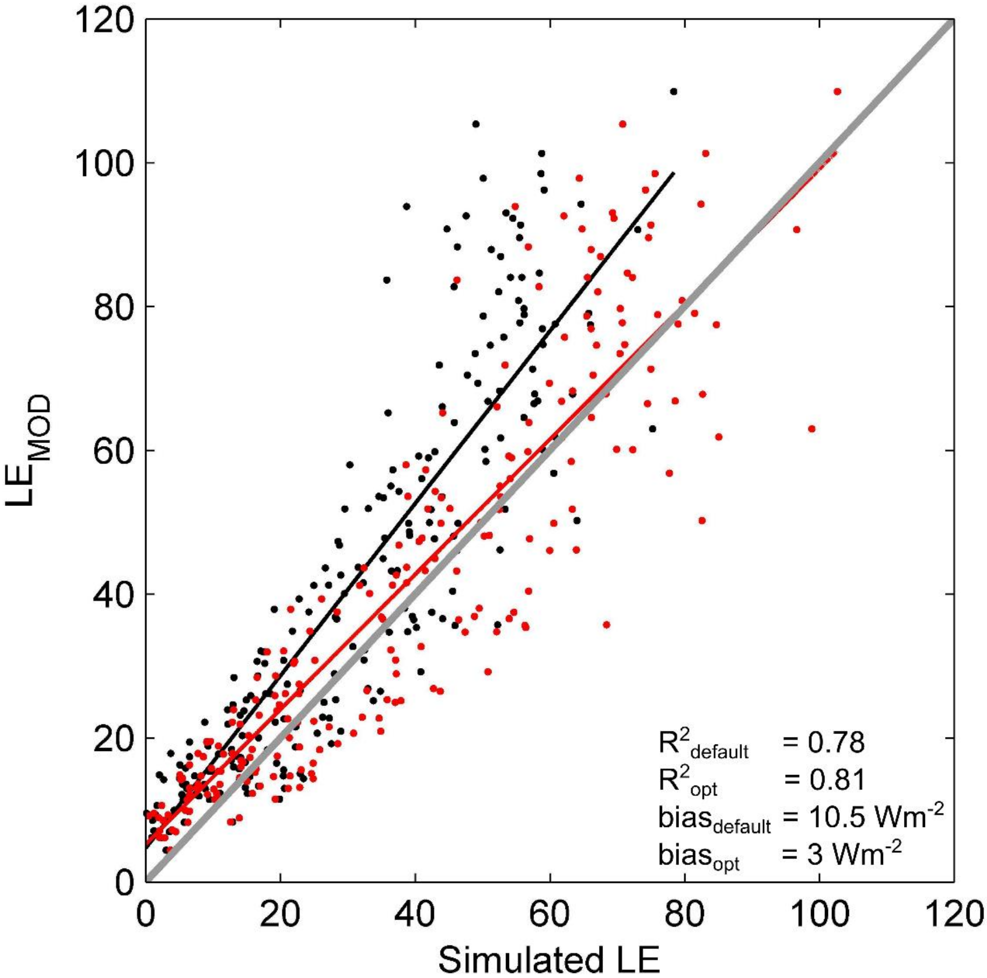

Figure 9. Spatially averaged monthly latent heat flux (*LE*) from MODIS, *default* and $macro_{opt}$ configurations over the Kennet catchment.

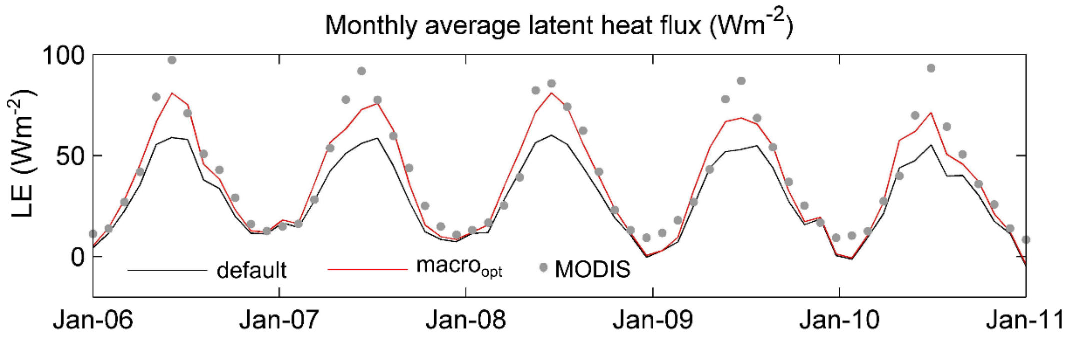

Supplementary materials

Figure S1. Saturation-pressure head relationship (May 2003 - December 2005) at Warren Farm measured fortnightly at 40 cm below land surface. (Source: Ned Hewett, CEH, personal communication).

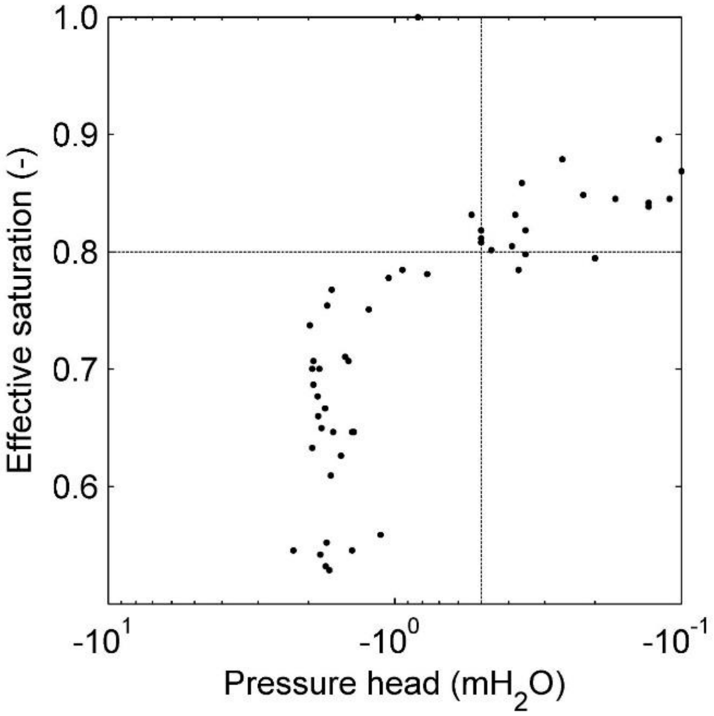

Figure S2. Sensitivity of the BC model parameters on the model performance in simulating $\Delta\theta$. Note that the parameters are considered one-at-a-time (OAT), and the vertical axis have different RMSE ranges.

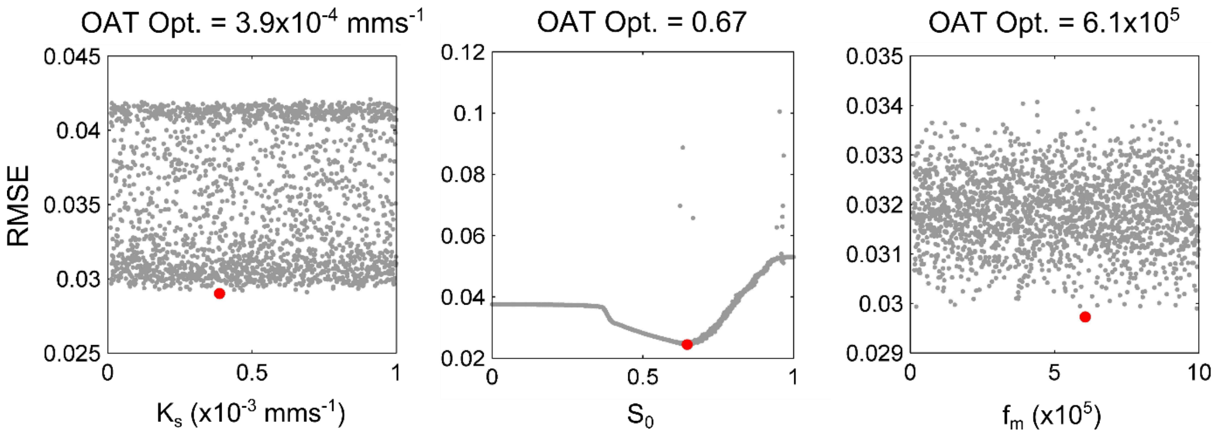

Towards a simple representation of chalk hydrology in land surface modelling

~~The effect of chalk representation in land surface modelling~~

Mostaquimur Rahman[1], Rafael Rosolem[1,2]

[1]Department of Civil Engineering, University of Bristol, Bristol, UK

[2]Cabot Institute, University of Bristol, Bristol, UK

Abstract

Modelling and monitoring of hydrological processes in the unsaturated zone of ~~the~~ chalk, ~~which is~~ a porous medium with fractures, is important to optimize water resources assessment and management practices in the United Kingdom (UK). However, incorporating the processes governing water movement through chalk unsaturated zone in a numerical model is complicated mainly due to the fractured nature of chalk that creates high-velocity preferential flow paths in the subsurface. ~~However, efficient simulations of water movement through chalk unsaturated zone is difficult mainly due to the fractured nature of chalk, which creates high-velocity preferential flow paths in the subsurface.~~In general, flow through chalk unsaturated zone is simulated using dual-porosity concept, which often involves calibration of relatively large number of model parameters, potentially undermining applications to large regions. Therefore, this approach may be not be suitable for large-scale land surface modelling applications. ~~Complex hydrology in the chalk aquifers may also influence land surface mass and energy fluxes because processes in the hydrological cycle are connected via non-linear feedback mechanisms. In this study, it is hypothesized that explicit representation of chalk hydrology in a land surface model influences land surface processes by affecting water movement through the shallow subsurface. In order to substantiate this hypothesis,~~ In this study, a simplified ~~macroporosity~~ parameterization, namely the Bulk Conductivity (BC) model ~~is~~ is proposed for simulating hydrology in chalk unsaturated zone. This new parameterization is implemented in the Joint UK Land Environment Simulator (JULES) and~~,~~ ~~which~~ ~~is~~ applied to ~~on~~ a study area encompassing the Kennet catchment in the Southern UK. The simulation results are evaluated using field measurements and satellite remote sensing observations of various fluxes and states of~~in~~ the hydrological cycle (e.g., soil moisture, runoff~~,~~ and latent heat flux) at two distinct spatial scales (i.e., point and catchment). The results demonstrate that the inclusion of the BC model in JULES improves simulated land surface mass and energy fluxes over the chalk-dominated Kennet catchment. Therefore, the simple approach described in this study may be used to incorporate the flow processes through chalk unsaturated zone in large scale land surface modelling applications. ~~The results reveal the influence of representing chalk hydrology on land surface mass and energy balance components such as surface runoff and latent heat flux via subsurface processes (i.e., soil moisture dynamics) in JULES, which corroborates the proposed hypothesis.~~

Keywords: Chalk hydrology, macroporosity, land surface model~~ling~~, bulk conductivity model.

1. Introduction

Chalk can be described as a fine-grained porous medium traversed by fractures [*Price et al.*, 1993]. Previous studies showed that ~~T~~the unsaturated zone of the chalk aquifers plays an important role on groundwater recharge ~~various important processes (e.g., recharge) of the hydrological cycle~~ in the UK [e.g., *Lee et al.*, 2006; *Ireson et al.*, 2009]. Therefore, both monitoring [e.g., *Bloomfield*, 1997; *Ireson et al.*, 2006] and modelling [e.g., *Bakopoulou*, 2015; *Brouyère*, 2006; *Ireson and Butler*, 2011, 2013; *Sorensen et al.*, 2014] strategies have been adapted previously to understand the governing hydrological processes in the chalk unsaturated zone.

In chalk, the matrix provides porosity and storage capacity, while the fractures greatly enhance permeability [*Van den Daele et al.*, 2007]. Water movement through chalk matrix is slow due to its relatively high porosity (0.3-0.4) and low permeability (10^{-9}-10^{-8} ms^{-1}). A fractured chalk system, in contrast, conducts water at a considerably higher velocity because of relatively high permeability (10^{-5}-10^{-3} ms^{-1}) and low porosity (of the order 10^{-4}) of fractures [*Price et al.*, 1993].

Simulating water flow through the matrix-fracture system of chalk has been the subject of research for some time. Both conceptual [e.g., *Price et al.*, 2000; *Haria et al.*, 2003] and physics-based [e.g., *Mathias* ~~*Mathius*~~ *et al.*, 2006; *Ireson et al.*, 2009] models have been proposed previously to describe water flow through chalk unsaturated zone. The physics-based models mentioned above were developed based on dual-continua approach and required relatively large number of parameters that were calibrated via inverse modelling using observed soil moisture and matric potential data.

~~The aforementioned studies revealed the importance of representing the matrix-fracture flow nature in simulating subsurface hydrological processes in chalk-dominated aquifers.~~ In recent years, representation of chalk has ~~also~~ gained attention in land surface modelling. *Gascoin et al.* [2009] applied the Catchment Land Surface Model (CLSM) over the Somme River basin in northern France. A linear reservoir was included in the TOPMODEL based runoff formulation of CLSM to account for the contribution of chalk aquifers to river discharge. *Le Vine et al.* [2016] applied the Joint UK Land Environment Simulator (JULES [*Best et al.*, 2011]) over the Kennet catchment in southern England to evaluate the hydrological limitations of land surface models. In that study, two intersecting Brooks and Corey curves were ~~curve was~~ proposed, which allowed a dual curve soil moisture retention representation for the two distinct flow domains of chalk (i.e., matrix and fracture) in the model. Considering this dual Brooks and Corey curve, a three-dimensional groundwater flow model

(ZOOMQ3D [*Jackson and Spink*, 2004]) was coupled to JULES to demonstrate the strong influence of representing chalk hydrology and groundwater dynamics ~~flow~~ on simulated soil moisture and runoff.

The above mentioned studies illustrate the importance of ~~suggest that the~~ representing ~~ation of~~ chalk in ~~affects the hydrological processes simulated by~~ land surface modellings~~s~~. However, including chalk hydrology in large-scale land surface modelling using the contemporary dual-porosity concept can be complicated because this approach generally involves relatively large number of parameters. In this context, we propose a new parameterization, namely the Bulk Conductivity (BC) model as a first step towards a simple chalk representation suitable for land surface modelling. The BC model is included in JULES and evaluated at two distinct spatial scales (i.e., point and catchment). ~~Because the processes of the hydrological cycle are connected via non-linear feedback mechanisms [e.g., *Kollet and Maxwell*, 2008; *Rahman et al.*, 2014], the representation of water flow through the matrix-fracture system of chalk may also influence simulated land surface energy fluxes (e.g., latent heat flux), which has not yet been explicitly discussed. In this context, our hypothesis is that a consistent representation of water movement through chalk in a land surface model affects the exchange of mass and energy fluxes at the surface, which may be important to consider in water resources assessment and management practices (e.g., flood and drought prediction over chalk-dominated areas). In order to substantiate this hypothesis, a macroporosity parameterization, namely the *Bulk Conductivity* (BC) model is implemented in JULES and evaluated at two distinct spatial scales (i.e., point and catchment).~~ At the point-scale, the BC model is evaluated using ~~against~~ observed soil moisture data. The proposed model is then applied to ~~over~~ the Kennet catchment in the Southern England and the fluxes and states of the hydrological cycle are simulated for multiple years. The simulation results are evaluated using observed latent heat flux (LE) and runoff to assess the performance of the BC model in simulating land surface processes at the catchment scale. to demonstrate the importance of representing chalk hydrology, which supports the proposed hypothesis.

2. A model of flow through chalk unsaturated zone

In this study, the *Bulk Conductivity* (BC) model based on the work by *Zehe et al.* [2001] is incorporated in JULES to represent the flow of water through the fractured chalk unsaturated zone. According to this approach, if the relative saturation (S) exceeds a certain threshold (S_0) at a soil grid, the saturated hydraulic conductivity (K_s) is increased to a bulk saturated hydraulic conductivity (K_{sb}) as follows

$$K_{sb} = K_s + K_s f_m \frac{S - S_0}{1 - S_0} \qquad \text{if } S > S_0 \qquad (1)$$

with $S = \frac{\theta - \theta_r}{\theta_s - \theta_r}$

where f_m is a macroporosity factor (-), θ is soil moisture (m^3m^{-3}), θ_s is soil moisture at saturation (m^3m^{-3}), and θ_r is the residual soil moisture (m^3m^{-3}). Note that S ranges from zero in case of completely dry soils to one for fully wet soils.

At the first step of evaluation, the K_s, S_0 and f_m parameters are estimated based on existing literature to assess the performance of the uncalibrated BC model. In this uncalibrated BC model, K_s for chalk matrix is 16 mmd^{-1} according to *Le Vine et al.* [2016] for the catchment investigated in this study (Figure 1).

Equation 1 indicates that the onset of water flow through the fracture system of chalk is controlled by the threshold S_0. According to *Wellings and Bell* [1980], water flow through fractures dominates over matrix flow in chalk when the pressure head in soil becomes higher than -0.50 mH_2O. We consider a value of In this study, S_0 = 0.80 for the uncalibrated BC model, which is based on observed soil moisture-matric potential relationship in the study area (Figure S1).

In *Zehe et al.* [2001], f_m was defined as the ratio of the saturated water flow rate in all macropores in a model element to the corresponding value in soil matrix, which can be determined based on the density and length of fractures at small scales. In addition, f_m has also been considered as a calibration parameter previously [e.g., *Blume*, 2008; *Zehe et al.*, 2013]. In this study, we define f_m as a characteristic soil property reflecting the influence of fractures on soil water movement [*Zehe and Blöschl*, 2004], and estimate it from the relative difference of permeability between chalk matrix and fractured chalk system that can be of the order 10^4-10^6 according to *Price et al.* [1999]. Consequently, we consider a macroporosity factor of $f_m = 10^5$ for the uncalibrated BC model.

In the following step, the BC model parameters are optimized to minimize the differences between the variability of observed and simulated soil moisture. Price et al. [1999] argued that the K_s for chalk matrix is generally around 3-5 mmd^{-1} (3.5-5.8x10^{-5} mms^{-1}). In order to optimize the BC model performance, we consider a range of K_s = 0.8-86 mmd^{-1} (10^{-5}-10^{-3} mms^{-1}) for chalk matrix in this study. As mentioned earlier, S is zero for completely dry soils and one in case of fully wet soils. Therefore, we consider a range of 0-1.0 for S_0 to optimize the BC model. For f_m, a range of 10^4-10^6 is considered, which, as discussed earlier, is consistent with the relative difference between the permeability of fractured chalk and chalk matrix according to *Price et al* [1999].

We use the Root Mean Squared Error (RMSE) as the objective function to optimize the BC model parameters [e.g., *Ireson et al.*, 2009]

$$RMSE = \frac{1}{nd}\sum_{1}^{nd}\sqrt{\left(\frac{1}{nt-1}\sum_{2}^{nt}\left(\Delta\theta_{d,t}^{obs} - \Delta\theta_{d,t}^{sim}\right)^2\right)} \qquad (2)$$

where *nd* is the number of soil layers, *nt* is the number of soil moisture observations available for a layer *d*, $\Delta\theta^{obs}$ is the observed variability of soil moisture and $\Delta\theta^{sim}$ is the simulated variability of soil moisture. Note that we consider $\Delta\theta$ for this optimization because of its relevance to the water flux and recharge through chalk unsaturated zone [e.g., *Ireson and Butler*, 2011]. Latin hypercube technique [e.g., *McKay et al.*, 2016] is used to generate 2000 random samples for each BC model parameter within the respective range discussed above. We perform simulations using these random samples and calculate model performance (Equation 2) to select the optimum parameter values for the BC model (discussed in section 4.1).

~~In *Zehe et al.* [2001], f_m was defined as the ratio of the saturated water flow rate in all macropores in a model element to the corresponding value in soil matrix, which can be determined based on density and length of fractures at small scales. In addition, f_m has also been considered as a calibration parameter previously [e.g., *Blume*, 2008; *Zehe et al.*, 2013]. In this study, we define f_m as a characteristic soil property reflecting the influence of fractures on soil water movement [*Zehe and Blöschl*, 2004], and estimate it from the relative difference of permeability between chalk matrix and fractured chalk system that can be of the order 10^5 according to *Price et al.* [1999]. Consequently, we consider a macroporosity factor of $f_m = 10^5$ in this study.~~

3. Methods

3.1. Study area

The study area encompasses the Kennet catchment located in the Southern England with an area of about 1033 km^2 (Figure 1a). Generally, Kennet~~, in general,~~ is rural in nature with scattered settlements and has a maximum altitude of approximately 297 m (Above Ordnance Level). The River Kennet discharges into the North Sea through London. The major ~~Major~~ tributaries of this river are Lambourn, Dun, Enborne, and Foudry Brook. An average annual rainfall of approximately 760 mm was recorded in the catchment over a 40 year period from 1961-1990.

Solid geology of the Kennet catchment is dominated by chalk, which is overlain by thin soil layer. While lower chalk outcrops along the northern catchment boundary, progressively younger rocks are found in the southern part. In general, surface runoff production is very limited over the regions of the catchment where chalk outcrops. The flow regime shows a distinct characteristics of slow response to groundwater held within the chalk aquifer [*Le Vine et al.*, 2016]. According to *Ireson and Butler* [2013], the unsaturated zone of chalk shows slow drainage over summer and bypass flow during wet periods in this catchment.

3.2. Field measurements and remotely sensed data

Table 1 summarizes the field measurements and remote sensing data used in this study. We use *in-situ* soil moisture and runoff measurements along with remotely sensed LE ~~latent heat flux (*LE*)~~ data to assess model performance in simulating the mass and energy balance components of the hydrological cycle. Point scale soil moisture measurements at two adjacent sites (~20 m apart) at the Warren Farm (Figure 1) were provided by Centre for Ecology and Hydrology (CEH). A Didcot neutron probe was used at these locations to measure fortnightly soil moisture at different depths below land surface (10 cm apart down to 0.8 m, 20 cm apart between 0.8-2.2 m, and 30 cm apart between 2.2-4.0 m) [*Hewitt et al.*, 2010].

The National River Flow Archive (NRFA) coordinates discharge measurements from the gauging station networks across UK. These networks are operated by the Environmental Agency (England), Natural Resources Wales, ~~the~~ Scottish Environment Protection Agency, and Rivers Agency (Northern Ireland). We use discharge measurement provided by NRFA to calculate the runoff ratio over the Kennet catchment in this study.

The MOD16 product of the Moderate Resolution Imaging Spectroradiometer (MODIS) is a part of NASA/EOS project that provides estimation of global terrestrial LE. The LE estimation from MOD16 is based on remotely sensed land surface data [e.g., *Mu et al.*, 2007]. In this study, the 8-day and monthly LE data products from MODIS is used to evaluate the model’s performance in simulating land surface energy fluxes.

3.3. Land surface model

In this study, we use the Joint UK Land Environment Simulator (JULES [e.g., *Best et al.*, 2011; *Clark et al.*, 2011]) version 4.2. JULES is a flexible modelling platform with a modular structure aligned to various physical processes developed based on the Met Office Surface Exchange Scheme (MOSES [e.g., *Cox et al.*, 1999; *Essery et al.*, 2003]). Meteorological data including precipitation, incoming short- and longwave radiation, temperature, specific humidity, surface pressure, and wind speed are required to drive JULES. Each grid box in JULES can comprise nine surface types (broadleaf trees, needle leaf trees, C3 grass, C4 grass, shrubs, inland water, bare soil, and ice) represented by respective fractional coverage. Each surface type is represented by a tile and a separate energy balance is calculated for each tile.

Subsurface heat and water transport equations are solved based on finite-difference approximation in JULES as described in *Cox et al.* [1999]. Moisture transport in the subsurface is described by the finite difference form of Richards’ equation. The vertical soil moisture flux is calculated using the Darcy’s law. While the top boundary condition to solve the Richards’ equation is infiltration at soil surface, the bottom boundary condition in JULES is free drainage that contributes to subsurface runoff.

Surface runoff is calculated by combining the equations of throughfall and grid box average infiltration in JULES. In order to direct the generated runoff to a channel network, river routing is implemented based on the discrete approximation of one-dimensional kinematic wave equation [e.g., *Bell et al.*, 2007]. In this approach, river network is derived from the digital elevation model (DEM) of the study area and different wave speeds are applied to surface and subsurface runoff components and channel flows [e.g., *Bell and Moore*, 1998]. A return flow term accounts for the transfer of water between subsurface and land surface [e.g., *Dadson et al.*, 2010, 2011].

3.4. Model configurations and input data

~~*3.4.1. Point scale*~~

~~At the point scale, JULES is configured to simulate the mass and energy fluxes at Warren Farm (Figure 1). A total subsurface depth of 5 m is considered in the model with a vertical discretization ranging from 10 cm at the land surface to 50 cm at the bottom of the model domain. Note that this discretization is consistent with the soil moisture measurement depths mentioned in section 3.2. The vegetation type is implemented as C3 grass using the default parameters in JULES. The soil hydraulic properties are estimated based on texture (Table 2), which is predominantly loamy at Warren Farm. The saturation-pressure head relationship is described using the Van Genuchten [*Van Genuchten*, 1980] model with parameter values (Table 2) obtained from *Schaap and Leij* [1998] in the model.~~

~~Point scale simulations were performed over 2 consecutive years from 2003-2005 at an hourly time step. Except for precipitation, hourly atmospheric forcing data to drive JULES was obtained from an automatic weather station operated by the CEH at Warren Farm. In order to estimate hourly precipitation data to run JULES, rain gauge measurements by the Met Office [*Met Office*, 2006] were used. Inverse distance interpolation technique [e.g. *Garcia et al.*, 2008; *Ly et al.*, 2013] was applied on rainfall measurements from 13 gauges closest to Warren Farm (distance varies from 25-60 km) to obtain hourly precipitation for the point scale simulations.~~

3.4.2. Catchment scale

At the catchment scale, JULES is configured over the study area (Figure 1) with a uniform lateral grid resolution of 1 km with 70 x 40 cells in x and y dimensions, respectively. The vertical discretization is identical to that of the point scale simulations described in the previous section. Spatially distributed vegetation type information for the study area (Figure 1b) is obtained from the Land Cover Map 2007 (LCM2007) dataset [e.g., *Morton et al.*, 2011]. Harmonized World Soil Database (HWSD) from the Food and Agricultural Organization of UNO (FAO) is used to obtain the texture of different soil types in the region (Figure 1c). Van Genuchten model, with parameter values (Table 2) obtained from *Schaap and Leij* [1998] is used to represent the saturation-pressure head relationship for different soil types, which is identical to the point scale simulations.

Simulations were performed over 5 consecutive years from 2006-2011 at the catchment scale. Note that the simulation periods of catchment and point scale (2003-2005) does not coincide due to the availability of soil moisture measurements described in section 3.2. Spatially distributed meteorological data from the Climate, Hydrology, and Ecology research Support System (CHESS) was used to obtain the atmospheric forcing to drive JULES. The CHESS data includes 1 km resolution gridded daily meteorological variables [*Robinson et al.*, 2015]. This daily data is downscaled using a disaggregation technique described in *Williams and Clark* [2014] to obtain hourly atmospheric forcing. The flow direction required for river routing is extracted from the USGS HydroSHEDS digital elevation data [*Lehner et al.*, 2008].

3.5. Setup of numerical experiments

We consider two different model configurations, namely, *default* and *macro* (Figure 2), to explore the influence of chalk hydrology on simulated land surface processes in JULES. The *default* configuration corresponds to the standard parameterizations of JULES that does not

~~represent chalk hydrology in the model. In this configuration, each soil column in JULES is considered to be vertically homogeneous with the soil properties defined in Table 2, which is motivated by the Met Office JULES Global Land 4.0 configuration described in *Walters et al.* [2014]. The *macro* configuration, in contrast, explicitly represents chalk hydrology in the model. The *macro* setup modifies the *default* configuration by applying chalk hydraulic properties (Table 3) from 30 cm below land surface to the bottom of the model domain (i.e. 500 cm). The BC model is applied in the chalk layers (30-500 cm) to simulate water flow in the *macro* configuration. Therefore, soil columns in the model can be divided into topsoil (0-30 cm) and chalk (30-500 cm) in *macro*. Note that except for this inclusion of chalk, *default* and *macro* configurations are identical in terms of model set up and input data.~~

~~The topsoil depth of 30 cm is defined based on several augured soil samples collected during a field campaign at Warren Farm in 2015 (Figure 2). This depth is corroborated by additional information from the British Geological Survey (BGS) operated borehole records (http://www.ukso.org/pmm/soil_depth_samples_points.html), which show that topsoil depths vary from 10-40 cm over the study area. We therefore apply the *macro* configuration assuming a spatially homogeneous 30 cm topsoil depth for both point and catchment scale simulations.~~

In this study, simulations are performed at two distinct spatial scales, namely point and catchment. At the point scale, JULES is configured to simulate the mass and energy fluxes at the Warren Farm site (Figure 1a). A total subsurface depth of 5 m is considered in the model with a vertical discretization ranging from 10 cm at the land surface to 50 cm at the bottom of the model domain. Note that this discretization is consistent with the soil moisture measurement depths mentioned in section 3.2. The vegetation type is implemented as C3 grass using the default parameters in JULES. Point scale simulations were performed over 2 consecutive years from 2003-2005 at an hourly time step. Except for precipitation, hourly atmospheric forcing data to drive JULES was obtained from an automatic weather station operated by the CEH at Warren Farm. In order to estimate hourly precipitation data to run JULES, rain gauge measurements from the Met Office [*Met Office*, 2006] were used. Inverse distance interpolation technique [e.g. *Garcia et al.*, 2008; *Ly et al.*, 2013] was applied on rainfall measurements from 13 gauges closest to Warren Farm (distance varies from 25-60 km) to obtain hourly precipitation for the point scale simulations.

At the catchment scale, JULES is configured over a study area encompassing the Kennet catchment (Figure 1a) considering a uniform lateral grid resolution of 1 km with 70 x 40 cells in x and y dimensions, respectively. The total subsurface depth and vertical discretization are identical to those of the point scale simulations. Spatially distributed vegetation type information for the study area (Figure 1b) is obtained from the Land Cover Map 2007 (LCM2007) dataset [*Morton et al.*, 2011]. Simulations were performed over 5 consecutive years from 2006-2011 at the catchment scale. Note that the simulation periods of catchment and point scale (2003-2005) does not coincide due to the availability of soil moisture measurements described in section 3.2. Spatially distributed meteorological data from the Climate, Hydrology and Ecology research Support System (CHESS) was used to obtain the atmospheric forcing to drive JULES at the catchment scale. The CHESS data includes 1 km resolution gridded daily meteorological variables [*Robinson et al.*, 2015]. This daily data is downscaled using a disaggregation technique described in *Williams and Clark* [2014] to obtain hourly atmospheric forcing. The flow direction required for river routing is extracted from the USGS HydroSHEDS digital elevation data [*Lehner et al.*, 2008].

We estimate the soil hydraulic properties based on texture (Table 2). At the point scale, loam soil is dominant at the Warren Farm site. At the catchment scale, the Harmonized World Soil Database (HWSD) from the Food and Agricultural Organization of UNO (FAO) is used to obtain the texture of different soil types over Kennet (Figure 1c). The saturation-pressure head relationship for different soil types is described using the Van Genuchten [*Van Genuchten*, 1980] model with parameter values (Table 2) obtained from *Schaap and Leij* [1998].

Table 3 summarizes the hydraulic properties for chalk used in this study. These properties are obtained based on existing literature as a first step when evaluating the uncalibrated BC model. The BC model parameters are subsequently optimized to minimize the differences between observed and simulated $\Delta\theta$.

In this study, we consider two different model configurations, namely *default* and *macro* (Figure 2). The *default* configuration corresponds to the standard parameterizations of JULES that does not represent chalk hydrology in the model. In this configuration, each soil column in JULES is considered to be vertically homogeneous with the soil properties defined in Table 2, which is motivated by the Met Office JULES Global Land 4.0 configuration described in *Walters et al.* [2014]. The *macro* configuration, in contrast, explicitly represents chalk by applying the BC model starting at 30 cm below land surface to the bottom of the model domain (i.e. 500 cm). Therefore, the soil column in the *macro* configuration can be divided into topsoil (0-30 cm) and chalk (30-500 cm) in *macro*. Note that except for this inclusion of chalk, *default* and *macro* configurations are identical in terms of model set up and input data.

The topsoil depth of 30 cm in the *macro* configuration is defined based on several augured soil samples collected during a field campaign at Warren Farm in 2015 (Figure 2). This depth is corroborated by additional information from the British Geological Survey (BGS) operated borehole records (http://www.ukso.org/pmm/soil_depth_samples_points.html), which show that topsoil depths vary from 10-40 cm over the study area. We therefore apply the *macro* configuration assuming a spatially homogeneous topsoil depth of 30 cm for both point and catchment scale simulations.

4. Results and discussion

4.1. Point scale simulations

At the point scale, the simulation results are evaluated using soil moisture observations at the Warren Farm site. Figure 3a compares observed and simulated soil moisture (θ) from the *default* and *macro* configurations at 2 m below land surface. Note that the *macro* configuration uses the chalk hydraulic parameters collected from existing literature (Table 3). This figure shows that the *default* configuration underestimates θ throughout the simulation period, which is improved remarkably in case of *macro*. Figure 3b plots observed and simulated soil moisture variability ($\Delta\theta$) from the *default* and *macro* configurations at the Warren Farm site. In general, both configurations show discrepancies with observed $\Delta\theta$ with *macro* showing relatively better model performance.

The results show that despite the *macro* configuration improves simulated θ, it shows considerable discrepancies with observed $\Delta\theta$, which is consistent throughout the whole chalk profile (results from other model layers are not shown). In order to minimize the differences between observed and modelled $\Delta\theta$ from the *macro* configuration, we optimize the BC model following the methodology described in section 2. The optimization results are summarized in Figure 4. Note that for each combination considered in the optimization, 2000 model runs were performed using randomly sampled parameters as discussed in section 2. Figure 4 presents the results from the model runs yielding the lowest RMSE.

The RMSE between observed and simulated $\Delta\theta$ for the model configurations considered in the optimization is shown in Figure 4a. This figure illustrates that the RMSE of the *default* configuration is larger than that of *macro*, indicating better model performance in reproducing $\Delta\theta$ for the latter. Therefore, it appears that the uncalibrated BC model (i.e., the *macro* configuration) is better in reproducing soil moisture variability compared to ~~the~~ *default* ~~configuration~~. Figure 4b, c and d presents the BC model parameter values from the model run producing the lowest RMSE for each configuration. Concerning single BC model parameters, Figure 4a shows that optimizing S_0 results in a 16% reduction of RMSE compared to the *macro* configuration. Optimizing K_s marginally improves model performance, which is observed from a slightly lower (4%) RMSE than *macro*. Optimizing both K_s and S_0 simultaneously results in the largest reduction (24%) of RMSE compared to *macro*.

Additionally, Figure 4 suggests that the sensitivity of S_0 on the model performance in simulating $\Delta\theta$ is substantially higher compared to K_s and f_m, which is corroborated by the sensitivity of the individual model parameters (Figure S2). Figure 4a also reveals the interesting fact that the RMSE from the configuration with optimized K_s and S_0 is identical to that of the one ~~the one~~ with ~~optimized~~ all 3 parameters optimized simultaneously (i.e., K_s, S_0 and f_m). Therefore, we select the *macro* configuration with optimized K_s and S_0 ($macro_{opt}$ hereafter) to simulate chalk hydrology over the study area.

~~Figure 3 shows observed and simulated volumetric soil moisture from the *default* model configuration at Warren Farm from 2003-2005. This figure shows that simulated soil moisture at shallow soil layers (up to 50 cm) compares reasonably well with the observed data. However, in the deeper layers, the model considerably underestimates soil moisture. Figure 4 compares observed and simulated volumetric soil moisture from the *macro* configuration at Warren Farm over the simulation period. This figure shows that especially in the deeper soil layers, the agreement between observed and simulated soil moisture improves remarkably relative to the *default* configuration throughout the simulation period. Notice again that the *default* and *macro* configurations are identical in terms of model setup and inputs except for the consideration of chalk. Therefore, the differences in soil moisture~~

~~simulations between the two model configurations can be attributed to the representation of chalk hydrology in JULES.~~

Figure 5 compares $\Delta\theta$ from the *macro*$_{opt}$ configuration ($\Delta\theta_{opt}$) with observed soil moisture variability ($\Delta\theta_{obs}$). As mentioned earlier, $\Delta\theta_{default}$ and $\Delta\theta_{macro}$ show considerable discrepancies with $\Delta\theta_{obs}$ while the *macro* configuration exhibits relatively better performance. Figure 5 illustrates that the overall agreement between observed and simulated $\Delta\theta$ improves substantially in case of *macro*$_{opt}$ compared to *default* and *macro*, which is pronounced especially in the deeper chalk layers. Therefore, this figure indicates that the performance of the BC model in simulating $\Delta\theta$ is further improved by optimizing the K_s and S_0 parameters at the Warren Farm site.

In order to assess the model performance in simulating soil moisture over the entire ~~chalk profile~~column, ~~Figure 5 presents t~~The relative bias ($\Delta\mu$, see Appendix) of simulated ~~soil moisture~~θ from the *default* and *macro*$_{opt}$ ~~two model~~ configurations at Warren Farm for various depth ranges are shown in Figure 6. In the soil layers (0-30 cm), θ from the two configurations are comparable with ~~both~~ the *default* ~~and *macro*~~ ~~configurations~~ showing slightly lower mean relative bias ($\Delta\mu_{mean}$) of -0.03 ~~reproduces soil moisture reasonably well with the latter showing slightly better~~ than *macro*$_{opt}$ ($\Delta\mu_{mean}$ = -0.09). ~~agreement with observations.~~ However, in the chalk layers (30-500 cm), *default* ~~fails to reproduce the soil moisture dynamics efficiently,~~ simulates~~ing~~ substantially drier~~dry~~ conditions, corresponding to ~~which are observed from the mean relative bias ($\Delta\mu_{mean}$) of~~ $\Delta\mu_{mean}$ ≤~~>~~ -0.28~~0.28 for this configuration~~. In contrast, the *macro*$_{opt}$ ~~*macro*~~ configuration considerably ~~remarkably~~ improves the agreement between the simulated and ~~with the~~ observed θ ~~soil moisture profile~~ in the chalk layers with ~~the largest calculated~~ $\Delta\mu_{mean}$ ~~=~~≥ -0.05~~-0.02~~. Therefore, the results indicate that the inclusion of the BC model in JULES improves the performance of overall soil moisture simulation (both θ and $\Delta\theta$) at Warren Farm especially in the chalk layers.

The drainage flux through the bottom of soil column (d_b) of a land surface model can be considered as the potential recharge flux to groundwater [e.g., *Sorensen et al.*, 2014]. ~~Therefore, the inclusion of the BC model in JULES appears to improve the performance of overall soil moisture simulation at Warren Farm especially in the chalk layers.~~Figure ~~6~~7 compares the daily sum of ~~drainage through the bottom of the soil column (d_b)~~ from the *default* and $macro_{opt}$ configurations at the Warren Farm site. The rainfall characteristics over the study period is shown in Figure ~~6~~7a. In Figure ~~6~~7b, the $macro_{opt}$ configuration shows considerable d_b during the colder months, while slow drainage prevails throughout the rest of the year. In contrast, the *default* configuration shows relatively high d_b in summer compared to the colder months. In general, the recharge rate through chalk unsaturated zone during the warmer periods of the year is lower than that in the winter months [*Wellings and Bell*, 1980; *Ireson et al.*, 2009]. Therefore, the $macro_{opt}$ configuration appears to be more consistent with the recharge mechanism in chalk compared to *default*.

In this section, the BC model was evaluated at the point scale. The results showed that in general, the *macro* configuration performs relatively better in simulating θ and $\Delta\theta$ compared to *default*. In order to improve the model performance even further, parameter optimization was performed to minimize the differences between observed and simulated $\Delta\theta$ at the point scale. In the next sections, the optimized model ($macro_{opt}$) is evaluated at the catchment scale.

~~In order to explore the reason of the discrepancies between simulated soil moisture from the two model configurations, Figure 6 shows S and water flux (w_f) profiles along with drainage through the bottom boundary (d_b) of *default* and *macro* for the entire simulation period. Figure 6b plots the contours of daily accumulated w_f through chalk (30-500 cm) over daily average S for the *macro* configuration (S_{macro}). Figure 6c shows S ($S_{default}$) and w_f through the same profile for the *default* configuration. A comparison between Figure 6b and 6c reveals that *default* is considerably drier compared to *macro* ($S_{default} < S_{macro}$) throughout the profile,~~

which is consistent with Figure 5. Figure 6b shows notable flux through the profile following strong precipitation events (Figure 6a), indicating fast water flow through subsurface in the *macro* configuration (especially in winter). The *default* configuration, on the other hand, shows relatively slower movement of water in the subsurface (Figure 6c).

According to the BC model, fracture flow in chalk is activated in a soil grid if S exceeds S_θ (defined as 0.80), which is achieved predominantly during winter following strong precipitation events because of the prevailing wet conditions. Therefore, the activation of fracture flow explains the fast water movement patterns after strong precipitation events observed in Figure 6b. This result is consistent with *Ireson et al.* [2009], who showed that fracture flow through chalk dominates at Warren Farm during wet periods. Compared to the *macro* configuration, *default* does not show fast water flow to the deeper soil layers because the latter does not represent the matrix-fracture flow nature of chalk in JULES.

Figure 6d compares daily sum of d_b from the two configurations. The *macro* configuration generally shows lower drainage compared to *default* with an exception in March 2003. Because of the gravity drainage lower boundary condition, water flow through the bottom of the model domain depends on K_s at the deepest soil layer in JULES. In chalk (*macro* configuration), K_s at the deepest soil layer is smaller compared to *default* (loam soil) especially when $S_\theta < 0.8$ (Equation 1), which explains the lower drainage flux in case of the *Chalk* configuration. The reason of higher d_b in *macro* compared to *default* in March 2003 is the strong precipitation events (Figure 6a) causing considerable fracture flow and $S > 0.8$ at the bottom of the model domain (Figure 6b).

Figure 6 outlines the differences in simulated subsurface processes by the two model configurations. Fracture flow in chalk is activated according to the BC approach during wet periods that allows recharge at deeper soil layers in *macro*, which is absent in case of the *default* configuration. Moreover, the *default* configuration generally shows higher drainage flux through the lower boundary compared to *macro*. The combination of relatively low recharge and high drainage through lower boundary is the reason of the drier conditions simulated by *default*. In contrast, the *macro* configuration is characterized by fast recharge at the deeper soil layers through fractures and slow drainage through the bottom because of considerably lower K_s compared to *default*, which is the reason of relatively higher simulated soil moisture by this configuration that compares well with observations.

Several previous studies have discussed the influence of root zone soil moisture on land surface mass and energy balance components [e.g., *Wetzel and Chang*, 1987; *Chen and Hu*, 2004]. Therefore, the differences in soil moisture from two configurations discussed above may affect the land surface mass and energy fluxes in the model. In order to investigate this effect, Figure 7 shows the difference between daily average latent heat flux (*LE*) time series from *default* and *macro* configurations ($LE_{default}$ and LE_{macro}, respectively) at Warren Farm over the simulation period. This figure shows that the *default* configuration generally simulates lower *LE* compared to *macro* especially in the warmer months of the year.

The underestimation of *LE* in Figure 7 can be attributed to the differences in simulated soil moisture by the two configurations (Figure 3 and 4). In winter, abundant soil moisture is available in both *default* and *macro* to meet the relatively low evapotranspiration (ET) demand due to the prevailing energy-limited conditions. Therefore, Figure 7 shows negligible differences between $LE_{default}$ and LE_{macro} in winter. However, in summer, the discrepancies between soil moisture from the two model configurations result in marked differences between $LE_{default}$ and LE_{macro} because of the increased ET demand, which is consistent with previous studies [e.g., *Rahman et al.*, 2016].

~~In this section, subsurface and land surface processes simulated by *default* and *macro* configurations are discussed at the point scale. The simulation results show notable differences in soil moisture and *LE* from the two configurations. Because the only difference between *default* and *macro* configurations is the representation of the chalk hydrology, it appears that a consistent representation of chalk in JULES affects land surface processes via subsurface hydrodynamics supporting our hypothesis. In the next section, we test this hypothesis regionally by evaluating the mass and energy fluxes of the hydrological cycle at the catchment scale.~~

4.2. Catchment scale simulations

In the previous section, it was observed that the *default* configuration generally underestimates θ compared to $macro_{opt}$. Previous studies have demonstrated the interconnections between shallow soil moisture and LE [e.g., *Chen and Hu*, 2004]. In order to assess the differences between the LE from the *default* and $macro_{opt}$ configurations at the catchment scale, Figure ~~7~~ 8 plots spatially averaged 8-day composites of LE from MODIS (LE_{MOD}) against the LE from these configurationse ~~*default* and $macro_{opt}$ configurations~~ ($LE_{default}$ and ~~LE_{macro}~~ LE_{opt}, respectively) over ~~the~~ Kennet ~~catchment~~. ~~In this figure, t~~The agreement between simulated LE and LE_{MOD} is evaluated using the coefficient of determination (R^2, see Appendix) and mean bias. Comparison between $LE_{default}$ and LE_{MOD} shows a coefficient of determination of $R^2_{default}$ = 0.78 and a mean bias of $bias_{default}$ = 10.5 Wm^{-2}. The agreement between simulated LE and LE_{MOD} improves in case of the $macro_{opt}$ ~~*macro*~~ configuration, which is reflected by an increased coefficient of determination of $R^2_{moptacro}$ = 0.81~~2~~ and a reduced mean bias of $bias_{opt}$ ~~of~~ = 3 Wm^{-2}.

Figure ~~8~~78 shows differences between $LE_{default}$ and LE_{opt} ~~LE_{macro}~~ especially for relatively high *LE*, indicating discrepancies especially during the warmer months of the year. Figure 9~~a~~

presents spatially averaged time series of monthly LE_{MOD}, $LE_{default}$ and LE_{opt} ~~LE_{macro}~~. This figure shows that the ~~negligible differences in *LE* from the two configurations during the colder months of the year, while~~ differences between $LE_{default}$ and LE_{opt} ~~LE_{macro}~~ increases substantially in summer compared to the colder months of the year, which is consistent with Figure ~~7~~8. Consequently, the *default* configuration underestimates *LE* ~~especially~~ in summer compared to LE_{MOD}, which is improved ~~when chalk hydrology is explicitly considered in JULES~~ in case of the $macro_{opt}$ ~~*macro*~~ configuration. In contrast, the differences between $LE_{default}$ and LE_{opt} ~~between~~ are negligible during the colder months of the year.

~~Figure 9b plots spatially averaged time series of daily $S_{default}$ and S_{macro} over the Kennet catchment. Note that average *S* at the first 8 vertical model layer (0-100 cm below land surface) is presented in this figure, which highlights the difference in root zone moisture content from the two model configurations. Figure 9b shows relatively lower *S* simulated by the *default* configuration compared to S_{macro}. In JULES, *LE* depends on surface conductance to evaporation, which is controlled by the mean soil moisture in the root zone. Therefore, the differences in $S_{default}$ and S_{macro} is consistent with the underestimation of *LE* by the *macro* configuration (Figure 9a). Note that despite the differences in *S* between the two configurations over the entire simulation period, Figure 9a shows significant *LE* differences only in summer. This is due to the prevailing energy limited conditions during the colder months over the region, which was discussed in the previous section. Figure 9 suggest that representing chalk hydrology in JULES considerably influences simulated *LE* by modifying shallow soil moisture at the catchment scale, also supporting our hypothesis.~~

Table 4 compares observed and simulated daily average runoff from the two model configurations over the Kennet catchment from 2006-2011. The runoff ratio (*RR*, see Appendix), which is equal to the mean volume of flow divided by the volume of precipitation [e.g., *Kelleher et al.*, 2015], assesses the partitioning of precipitation into runoff over the catchment. The *default* configuration (*RR* = 0.82) shows considerably higher *RR* compared to observation (*RR* = 0.40), indicating overestimation of runoff by the model. Including chalk hydrology in the model remarkably improves the agreement between observed and simulated mean runoff over the Kennet catchment, which is assessed from a runoff ratio of *RR* = 0.37~~8~~ for the $macro_{opt}$ ~~*macro*~~ configuration.

In Table 4, the relative bias (Δμ) of 1.04 between observed and simulated runoff from the *default* configuration again indicates the overestimation by the model. In comparison, $macro_{opt}$ ~~*macro*~~ shows a relative bias (Δμ = ~~-~~-0.05 ~~0.07~~), indicating improvement between observed and simulated mean runoff volume compared to *default*. The relative difference in standard deviation (Δσ, see Appendix) compares the variability ~~magnitude~~ of observed and simulated runoff in Table 4~~3~~. This comparison shows that the *default* configuration overestimates the variability of runoff over the Kennet catchment (Δσ = 2.04), which is improved in case of *macro* (Δσ = ~~0.56~~0.70).

It was demonstrated previously that the *default* configuration predicts lower evapotranspiration (ET) compared to $macro_{opt}$ over the Kennet catchment due to the differences in simulated *θ*. In JULES, moisture from soil and canopy is depleted to meet the ~~evapotranspiration (ET)~~ demand. Additionally, surface runoff generation depends on canopy water storage in the model [*Best et al.*, 2011]. Because of this connection between ET and surface runoff generation via canopy water storage, the differences in runoff demonstrated in Table 4 can be attributed to the disagreements between $LE_{default}$ and LE_{macro} (~~demonstrated in~~ Figure 8) due to the relatively drier conditions simulated by *default*.

~~In JULES, moisture from soil and canopy water storage is depleted to meet the ET demand. Additionally, surface runoff generation depends on canopy water storage in the model [*Best*~~

~~*et al.*, 2011]. Because of this connection between ET and surface runoff generation via canopy water storage, the differences in runoff demonstrated in Table 4 can be attributed to the disagreement between $LE_{default}$ and LE_{macro} demonstrated in Figure 9a. Therefore, it appears that *LE* in JULES is affected by the inclusion of chalk hydrology, which consequently influences surface runoff generation corroborating our hypothesis.~~

In this section, the BC model is evaluated using observed mass and energy fluxes over the Kennet catchment. The *default* configuration ~~default configurations~~ showed considerably low LE over the catchment, which was pronounced during the warmer period of the year. The agreement between observed and simulated LE was improved in case of the $macro_{opt}$ configuration compared to *default*. It was also observed that the overall runoff prediction was ~~also~~ improved by $macro_{opt}$ compared to *default*. Given its simplicity, our results indicate that the proposed parameterization is suitable for use in land surface modelling applications.

5. Summary and Conclusions

In this study, we proposed a simple parameterization~~we hypothesized that a consistent representation of chalk hydrology affects land surface mass and energy balance components via subsurface hydrodynamics simulated by a land surface model. In order to support this hypothesis~~, namely the ~~the~~ *Bulk Conductivity* (BC) model ~~that~~ to simulates water flow through the matrix-fracture system of chalk in large scale land surface modelling applications. This parameterization was implemented in the Joint UK Land Environment Simulator (JULES) and~~. This model was~~ applied to ~~on~~ the Kennet catchment located in the southern UK to simulate the mass and energy fluxes of the hydrological cycle for multiple years. Two model configurations, ~~namely~~ namely *default* and *macro* were considered with the latter ~~representing~~ using the BC model to simulate chalk hydrology~~ in JULES using the BC model~~.

The proposed BC model is a single continuum approach of modelling preferential flow [e.g., *Beven and Germann*, 2013] that involves only 2 parameters, namely macroporosity factor (f_m) and relative saturation threshold (S_0). Initially, these parameters along with the saturated hydraulic conductivity of the chalk matrix were estimated from existing literature. Finally, the BC model parameters were optimized to minimize the differences between observed and simulated soil moisture variability. Our results indicated that S_0 is the most influential parameter in the model when representing water movement through a soil-chalk column, followed by the saturated hydraulic conductivity of chalk matrix while f_m showed low sensitivity. Hence, the parameterization is further improved by optimizing both saturated hydraulic conductivity of chalk matrix and S_0 to minimize the differences between observed and simulated soil moisture variability.

The simulation results were evaluated using observed mass and energy fluxes both at point and catchment scales. The results demonstrated that the inclusion of the BC model in JULES improves simulated soil moisture variability at the point scale compared to a model configuration that does not represent chalk in the subsurface (i.e., the *default* configuration). At the catchment scale, it was illustrated that the proposed parameterization improves simulated latent heat flux and overall runoff compared to the *default* configuration. ~~The discrepancies between the measured and simulated fluxes and states can be improved by a comprehensive model calibration, which is out of the scope of this study and should be the subject of future research.~~

Note that the complexity of the BC model for simulating water flow through chalk unsaturated zone is substantially lower compared to more commonly used models for this purpose (e.g., dual-porosity models). Despite its simplicity, it appears that the proposed parameterization improves mass and energy fluxes simulated by JULES over the Kennet catchment. As mentioned previously, representing chalk hydrology in land surface models using the dual-porosity concept is complicated mainly due to the relatively large number of parameters involved in such approach. Therefore, the simplified parameterization proposed in this study may be useful for large-scale land surface modelling applications over chalk-dominated areas.

The results showed that JULES generally underestimates root zone soil moisture without a consistent representation of chalk hydrology. Consequently, *LE* is underestimated by the model without chalk representation. The effect of chalk hydrology was also observed on runoff, which was attributed to the interconnection between *LE* and runoff generation in the model. Therefore, representing the matrix-fracture flow nature of chalk in a land surface model affects land surface processes via shallow soil moisture dynamics, which supports the proposed hypothesis.

Habtes et al. [2010] argued that flood flow in chalky catchments is influenced by the hydrological processes in the unsaturated zone. Implementing the BC model in JULES, this study showed that representing chalk hydrology significantly affects subsurface and land surface mass and energy fluxes. Therefore, the matrix-fracture flow nature of the aquifer may be important to consider in flood forecasting in chalk-dominated catchments.

Leeper et al. [2011] discussed the influence of shallow soil moisture on simulated atmospheric processes over karst landscapes because of the subsurface-land surface connection in the terrestrial system. In this study, we demonstrated that considering chalk hydrology considerably affects land surface mass and energy fluxes via subsurface hydrodynamics. This effect may be important to consider in numerical weather prediction models over the regions dominated by chalk because of the karst behaviour of chalk aquifers [e.g., *MacDonald et al.*, 1998; *Hartmann et al.*, 2014].

~~*Le Vine et al.* [2016] argued that the deep-groundwater system in a chalk-dominated catchment may influence the mass and energy balance components of the hydrological cycle, which is not considered in this study. The reason for that is JULES simulates water flow at shallow subsurface considering free drainage lower boundary condition and does not allow lateral movement of water between the soil columns. The effect of groundwater dynamics can be represented in JULES by coupling a three-dimensional groundwater flow model [e.g., *Le Vine et al.*, 2016; *Maxwell and Miller*, 2005], which will be addressed in future.~~

Acknowledgements

We gratefully acknowledge the support by the "A MUlti-scale Soil moisture Evapotranspiration Dynamics study – AMUSED" project funded by Natural Environment Research Council (NERC) grant number NE/M003086/1. The authors would also like to thank Ned Hewitt and Jonathan Evans from the Centre for Ecology and Hydrology (CEH) for providing the data for the point-scale analyses at the Warren Farm. Finally, we would like to thank Miguel Rico-Ramirez (University of Bristol) for helping preparing the precipitation data from the rain gauge network used for the point-scale simulations, Thorsten Wagener (University of Bristol) for his valuable suggestions on model diagnostics, and Joost Iwema (University of Bristol) for helping with the soil samples collected during the 2015 field work campaign.

Appendix

Definition of Statistical Metrics

Coefficient of determination (R^2) for observation y = y1, …, yn and prediction f = f1, …, fn is defined as

$$R^2 = 1 - \frac{SS_{res}}{SS_{tot}}$$

where, SS_{res} is the residual sum of square and SS_{tot} is the total sum of square. SS_{res} and SS_{tot} are defined as

$$SS_{res} = \sum_{i=1}^{n}(y_i - f_i)^2 \qquad \text{and}$$

$$SS_{tot} = \sum_{i=1}^{n}(y_i - \bar{y})^2 \qquad \text{with } \bar{y} \text{ being the mean of y.}$$

Runoff ratio (RR) assesses the portion of precipitation that generates runoff over the catchment. RR is defined as

$$RR = \frac{\mu_{runoff}}{\mu_{rain}}$$

where μ_{runoff} is mean runoff and μ_{rain} is mean precipitation [e.g., *Kelleher et al.*, 2015].

Relative bias ($\Delta\mu$) between observed and simulated time series can be defined as

$$\Delta\mu = \frac{\mu_{mod} - \mu_{obs}}{\mu_{obs}}$$

where μ_{obs} and μ_{mod} are the mean of observed and simulated time series, respectively. While the optimal value of $\Delta\mu$ is zero, negative (positive) values indicate an underestimation (overestimation) by the model [e.g., *Gudmundsson et al.*, 2012].

Relative difference in standard deviation ($\Delta\sigma$) between observed and simulated time series can be defined as

$$\Delta\sigma = \frac{\sigma_{mod} - \sigma_{obs}}{\sigma_{obs}}$$

where σ_{obs} and σ_{mod} are the standard deviation of observed and simulated time series, respectively [e.g., *Gudmundsson et al.*, 2012].

References

Bakopoulou, C. (2015), Critical assessment of structure and parameterization of JULES land surface model at different spatial scales in a UK Chalk catchment, PhD thesis, Imperial College London, UK, available at: https://spiral.imperial.ac.uk:8443/handle/10044/1/28955.

Bell, V. A. and R. J. Moore (1998), A grid-based flood forecasting model for use with weather radar data: Part 1. Formulation, Hydrol. Earth Syst. Sc., 2, 265-281.

Bell, V. A., A. L. Key, R. G. Jones, and R. J. Moore (2007), Development of a high resolution grid-based river flow model for use with regional climate model output, Hydrol. Earth Syst. Sc., 11, 532-549.

Best, M. J., M. Pryor, D. B. Clark, G. G. Rooney, R. l. H. Essery, C. B. Ménard, J. M. Edwards, M. A. Hendry, A. Porson, N. Gedney, L. M. Mercado, S. Sitch, E. Blyth, O. Boucher, P. M. Cox, C. S. B. Grimmond, and R. J. Harding (2011), The Joint UK Land Environment Simulator (JULES), Model Description – Part 1: Energy and Water Fluxes, Geosci. Model Dev., 4, 677-699.

Beven, K., and P. Germann (2013), Macropores and water flow in soils revisited, Water Resour. Res., 49, 3071‐3092.

Bloomfield, J. (1997), The role of diagenesis in the hydrogeological stratification of carbonated aquifers: An example from the chalk at Fair Cross, Berkshire, UK, Hydrol. Earth Syst. Sc., 1, 19-33.

Blume, T. (2008), Hydrological processes in volcanic ash soils: measuring, modelling and understanding runoff generation in an undisturbed catchment, PhD thesis, Institut für Geoökologie, Universität Potsdam, Potsdam, Germany., available at: https://publishup.uni-potsdam.de/opus4-ubp/files/1524/blume_diss.pdf

Brouyère, S. (2006), Modelling the migration of contaminants through variably saturated dual-porosity, dual-permeability chalk, J. Contam, Hydrol., 82, 195-219.

Chen, X., and Q. Hu (2004), Groundwater influences on soil moisture and surface evaporation, J. Hydrol., 297, 285‑300.

Clark, D. B., L. M. Mercado, S. Sitch, C. D. Jones, N. Gedney, M. J. Best, M. Pryor, G. G. Rooney, R. L. H. Essery, E. Blyth, O. Boucher, R. J. Harding, C. Huntingford, and P. M. Cox (2011), The Joint UK Land Environment Simulator (JULES), Model Description – Part 2: Carbon Fluxes and Vegetation Dynamics, Geosci. Model Dev. 4, 701-722.

Cox, P. M., R. A. Betts, C. B. Bunton, R. L. H. Essery, P. R. Rowntree and J. Smith (1999), The impact of new land surface physics on the GCM simulation of climate and climate sensitivity, Clim. Dynam., 15, 183-203.

Dadson, S. J., I. Ashpole, P. Harris, H. N. Davies, D. B. Clark, E. Blyth, and C. M. Taylor (2010), Wetland inundation dynamics in a model of land surface climate: Evaluation in the Niger inland delta region, J. Geophys. Res., 115.

Dadson, S. J., V. A. Bell, and R. G. Jones (2011), Evaluation of a grid based river flow model configured for use in a regional climate model, J. Hydrol., 411, 238-250.

Dettinger, M. D., and H. F. Diaz (2000), Global characteristics of streamflow seasonality and variability, J. Hydrometeorol., 1, 289-310.

Essery, R., M. Best, and P. Cox (2001), MOSES 2.2 technical documentation (Hadley Centre technical note 30), Hadley Centre, Met Office, UK.

Garcia, M., C. D. Peters-Lidard, and D. C. Goodrich (2008), Spatial interpolation of precipitation in a dense gauge network for monsoon storm events in the southwestern United States, Water Resour. Res., 44.

Gascoin, S., A. Duchare, P. Ribstein, M. Carli, and F. Habtes (2000), Adaptation of a catchment-based land surface model to the hydrological setting of the Somme River basin (France), J. Hydrol., 368, 105-116.

Gudmundsson, L., T. Wagener, L. M. Tallaksen, and K. Engeland (2012), Evaluation of nine large-scale hydrological models with respect to the seasonal runoff climatology in Europe, Water Resour. Res., 48.

Gupta, H. V., H. Kling, K. K. Yilmaz, and G. F. Martinez (2009), Decomposition of the mean squared error and NSE performance criteria: implications for improving hydrological modelling, J. Hydrol., 377, 80-91.

~~Habtes, F., S. Gascoin, S. Korkmaz, D. Thiéry, M. Zribi, N. Amraoui, M. Carli, A. Ducharne, E. Leblois, E. Ledoux, E. Martin, J. Noilhan, C. Ottlé, and P. Viennot (2010), Multi-model comparison of a major flood in the groundwater-fed basin of the Somme River (France), Hydrol. Earth Syst. Sc., 14, 99-117.~~

Haria, A. H., M. G. Hodnett, and A. C. Johnson (2003), Mechanisms of groundwater recharge and pesticide penetration to chalk aquifer in southern England, J. Hydrol., 275, 122-137.

Hartmann, A., N. Goldscheider, T. Wagener, J. Lange, and M. Weiler (2014), Karst water resources in a changing world: Review of hydrological modeling approaches, Rev. Geophys., 52, 218–242, doi:10.1002/2013RG000443.

Hewitt, N., M. Robinson, and D. McNeil (2010), Pang and Lambourn hydrometric review 2009, Wallingford, NERC/Centre for Ecology and Hydrology, (CEH project number: C04076).

Ireson, A. M., S. A. Mathias, H. S. Wheater, A. P. Butler and J. Finch (2009), A model for flow in the chalk unsaturated zone incorporating progressive weathering, J. Hydrol., 365, 244-260.

Ireson, A. M. and A. P. Butler (2011), Controls on preferential recharge to chalk aquifers, J. Hydrol., 398, 109-123.

Ireson, A. M. and A. P. Butler (2013), A critical assessment of simple recharge models: application to the UK chalk, Hydrol. Earth Syst. Sc., 17, 2083-2096.

Ireson, A. M., H. S. Wheater, A. P. Butler, S. A. Mathias, J. Finch, and J. D. Cooper (2006), Hydrological processes in the chalk unsaturated zone – insight from an intensive field monitoring program, J. Hydrol., 330, 29-43.

Ireson, A. M., S. A. Mathias, H. S. Wheater, A. P. Butler, and J. Finch (2009), A model for flow in the chalk unsaturated zone incorporating progressive weathering, J. Hydrol., 365, 244-260.

Jackson, C. and Spink, A. (2004) User's Manual for the Groundwater Flow Model ZOOMQ3D, IR/04/140, British Geological Survey, Nottingham, UK.

Kelleher, C., T. Wagener, and B. McGlynn (2015), Model-based analysis of the influence of catchment properties on hydrologic partitioning across five mountain headwater subcatchments, Water Resour. Res., 51, 4109-4136.

Kling, H., M. Fuchs, and M. Paulin (2012), Runoff conditions in the upper Danube basin under an ensemble of climate change scenarios. Journal of Hydrology, Volumes 424-425, 6 March 2012, 264-277.

~~Kollet, S. J., and R. M. Maxwell (2008), Capturing the influence of groundwater dynamics on land surface processes using an integrated, distributed watershed model, Water Resour. Res., 44.~~

Lehner, B., K. Verdin, and A. Jarvis (2008), New global hydrography derives from spaceborne elevation data, EOS, Transactions, AGU, 89(10), 93-94.

Le Vine, N., A . Butler, N. McIntyre, and C. Jackson (2016), Diagnosing hydrological limitations of a land surface model: application of JULES to a deep-groundwater chalk basin, Hydrol. Earth Syst. Sc., 20, 143-159.

Lee, L. J. E., D. S. L. Lawrence, and M. Price (2006), Analysis of water-level response to rainfall and implications for recharge pathways in the chalk aquifer, SE England, J. Hydrol., 330, 604-620.

~~Leeper, R., R. Mahmood, and R. I. Quintanar (2011), Influence of karst landscape on planetary boundary layer atmosphere: A Weather Research Forecasting (WRF) model-based investigation, J. Hydrometeorol., 12, 1512-1529.~~

Ly, S., C. Charles, and A. Degré (2013), Different methods for spatial interpolation of rainfall data for operational hydrology and hydrological modeling at watershed scale. A review, Biotechnol. Agron. Soc. Environ. 17, 392-406.

~~MacDonald, A. M., L. J. Brewerton, and D. J. Allen (1998), Evidence of rapid groundwater flow and karst type behaviour in the chalk of Southern England, In: Robins, N. S. (ed.) *Groundwater pollution, aquifer recharge and vulnerability*, Geological Society, London, Special publications, 130, 95-106.~~

Mathias, S. A., A. P. Butler, B. M. Jackson, and H. S. Wheater (2006), Transient simulations of flow and transport in the chalk unsaturated zone, J. Hydrol., 330, 10-28.

~~Maxwell, R.M. and N.L. Miller (2005), Development of a coupled land surface and groundwater model, J. Hydrometeorol., 6(3), 233-247.~~

~~Maxwell, R. M., F. K. Chow, S. J. Kollet (2007), The groundwater-land-surface-atmosphere connection: Soil moisture effects on the atmospheric boundary layer in fully-coupled simulations, Adv. Water Resour., 30, 2447–2466.~~

Met Office (2006), UK hourly rainfall data, Part of the Met Office Integrated Data Archive System (MIDAS), NCAS British Atmospheric Data Centre, 21 March 2016, http://catalogue.ceda.ac.uk/uuid/bbd6916225e7475514e17fdbf11141c1.

Morton, D., C. Rowland, C. wood, L. Meek, C. Marston, G. Smith, R. Wadsworth, and I. C. Simpson (2011), Final report for LCM2007 – the new UK Land Cover Map (CS technical report no 11/07), Centre for Ecology and Hydrology, UK.

Mu, Q., F. A. Heinsch, M. Zhao, and S. W. Running (2007), Development of a global evapotranspiration algorithm based on MODIS and global meteorology data, Remote Sens. Environ., 111, 519-536.

Price, A., R. A. Downing, and W.M. Edmunds (1993), The chalk as an aquifer. In: Downing, R. A., M. Price, and G. P. Jones *The hydrogeology of the chalk of north-west Europe*. Oxford: Claredon Press. 35-58.

Price, M., R. G. Low, and C. McCann (2000), Mechanisms of water storage and flow in the unsaturated zone of chalk aquifer, J. Hydrol., 54-71.

~~Rahman, M., M. Sulis, and S. J. Kollet (2014), The concept of dual-boundary forcing in land surface-subsurface interactions of the terrestrial hydrologic and energy cycles, Water Resour. Res., 50, 8531-8548.~~

~~Rahman, M., M. Sulis, and S. J. Kollet (2016), Evaluating the dual-boundary forcing concept in subsurface- land surface interactions of the hydrological cycle, Hydrol. Process.~~

Rawls, W. J., D. L. Brankensiek, and K. E. Saxton (1982), Estimation of soil water properties, Trans. ASAE, 25(5), 1316–1320.

Robinson, E. L., E. Blyth, D. B. Clark, J. Finch, and A. C. Rudd (2015), Climate hydrology and ecology research support system potential evapotranspiration dataset for Great Britain (1961- 2012) [CHESS-PE], NERC-Environmental Information Data Centre.

Schär C., D. Lüthi, U. Beyerle, and E. Heise (1999), A soil precipitation feedback: A process study with a regional climate model, J. Clim., 12, 722–741.

Schaap, M. G., and F. J. Leij (1998), Database-related accuracy and uncertainty of pedotransfer functions, Soil Sci., 163(10), 765-779.

Sorensen, J. P. R., J. W. Finch, A. M. Ireson, and C. R. Jackson (2014), Comparison of varied complexity models simulating recharge at the field scale, Hydrol. Process., 28, 2091-2102.

Van den Daele, G. F. A., J. A. Barker, L. D. Connell, T. C. Atkinson, W. G. Darling, and J. D. Cooper (2007), J. Hydrol., 342, 157-172.

Van Genuchten, M. Th. (1980), A closed-form equation for predicting the hydraulic conductivity of unsaturated soils, Soil Sci. Soc. Am. J., 44, 892‑898.

Walters, D. N., K. D. Williams, I. A. Boutle, A. C. Bushell, J. M. Edwards, P. R. Field, A. P. Lock, C. J. Morcrette, R. A. Stratton, J. M. Wilkinson, M. R. Willett, N. Bellouin, A. Bodas-Salcedo, M. E. Brooks, D. Copsey, P. D. Earnshaw, S. C. Hardiman, C. M. Harris, R. C. Levine, C. MacLachlan, J. C. Manners, G. M. Martin, S. F. Milton, M. D. Palmer, M. J. Roberts, J. M. Rodríguez, W. J. Tennant, and P. L. Vidale (2014), The Met Office unified model global atmosphere 4.0 and JULES global land 4.0 configurations, Geosci. Model Dev., 7, 361-386.

Welliings, S. R., and J. P. Bell (1980), Movement of water and nitrate in the unsaturated zone of upper chalk near Winchester, Hants., England, J. Hydrol, 48, 119-136.

~~Wetzel P. J., and J.-T. Chang (1987), Concerning the relationship between evapotranspiration and soil moisture. J. Clim. Appl. Meteorol., 26, 18‑27.~~

Williams, K., and D. Clark (2014), Disaggregation of daily data in JULES (Hadley Centre technical note 96), Hadley Centre, Met Office, UK.

Zehe, E. and G. Blöschl (2004), Predictability of hydrologic response at the plot and catchment scales: Role of initial conditions, Water Resour. Res, 40.

Zehe, E., T. Maurer, J. Ihringer, and E.Plate (2001), Modeling water flow and mass transport in a loess catchment, Phys. Chem. Earth (B), 26, 487-507.

Zehe, E., U. Ehret, T. Blume, A. Kleidon, U. Scherer, and M. Westhoff (2013), A thermodynamic approach to link self-organization, preferential flow and rainfall-runoff behaviour, Hydrol. Earth Syst. Sc., 17, 4297-4322.

Tables

Table 1. Field measurements and remote sensing data.

Data	Spatial scale	Temporal extent	Frequency	Source
Soil moisture	Point[a]	2003-2005	15 day	N. Hewitt (CEH)
Latent heat flux	Global	2006-2011	8 day, 1 month	MODIS
Discharge	Point[b]	2006-2011	1 day	NRFA

[a]Measured at Warren Farm.
[b]Locations are shown in Figure 1a.

Table 2. Hydraulic properties for different soil types (refer to Figure 1c). Saturated hydraulic conductivity (K_s) and porosity data are obtained from *Rawls et al.* [1982]. The Van Genuchten parameters are acquired from *Schaap and Leij* [1998].

Texture	K_s (ms^{-1})	Porosity (-)	α (m^{-1})	n (-)
Loam	$3.7x10^{-6}$	0.463	3.33	1.56
Silt loam	$2.0x10^{-6}$	0.50	1.2	1.39
Clay	$1.7x10^{-7}$	0.475	2.12	1.2

~~Table 3. Hydraulic properties of chalk.~~

~~Properties~~	~~Value~~	~~Source~~
~~K_s (ms^{-1})~~	~~$1.85x10^{-7}$~~	~~Price et al., 1993~~
~~Porosity (-)~~	~~0.40~~	~~Price et al., 1993~~
~~α (m^{-1})~~	~~3.4~~	~~Le Vine et al., 2016~~
~~n (-)~~	~~1.4~~	~~Le Vine et al., 2016~~

Table 3. Hydraulic properties of chalk

	Unoptimized		Optimized value
Properties	Value	Source	
K_s (md^{-1})	16	Le Vine et al., 2016	15
S_0 (-)	0.8	Observations	0.67
f_m (-)	$1x10^5$	Price et al., 1993	$6.1x10^5$
α (m^{-1})	3.0	Le Vine et al., 2016	-
n (-)	1.4	Le Vine et al., 2016	-

Table 4. Comparison between observed and simulated daily average runoff from the two configurations over the Kennet catchment.

Metric	Observed	Simulated (*default*)	Simulated (*macro*)
RR	0.40	0.82	0.37~~8~~
Δμ	-	1.04	-0.05~~-0.07~~
Δσ	-	2.04	0.70~~0.56~~

Figures

Figure 1. Location (a), vegetation cover (b), and soil texture (c) over the study area. The red line in (a) outlines the Kennet catchment boundary, while the river network is shown in blue. The black triangle in (a) shows the location of the discharge gauging station at the catchment outlet while the black square corresponds to Warren Farm location where point-scale simulations are carried out. The shaded area in (c) represents the location of chalk in the catchment.

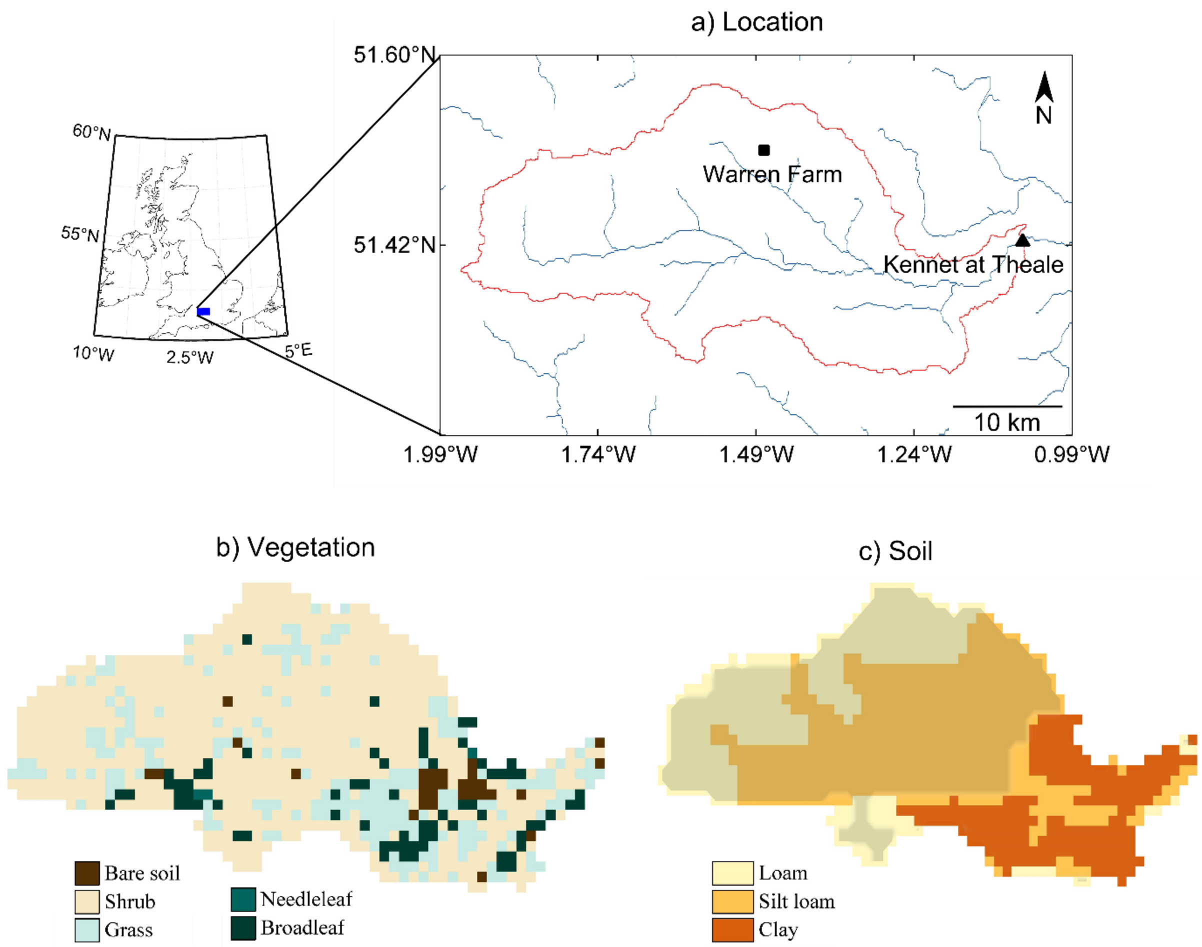

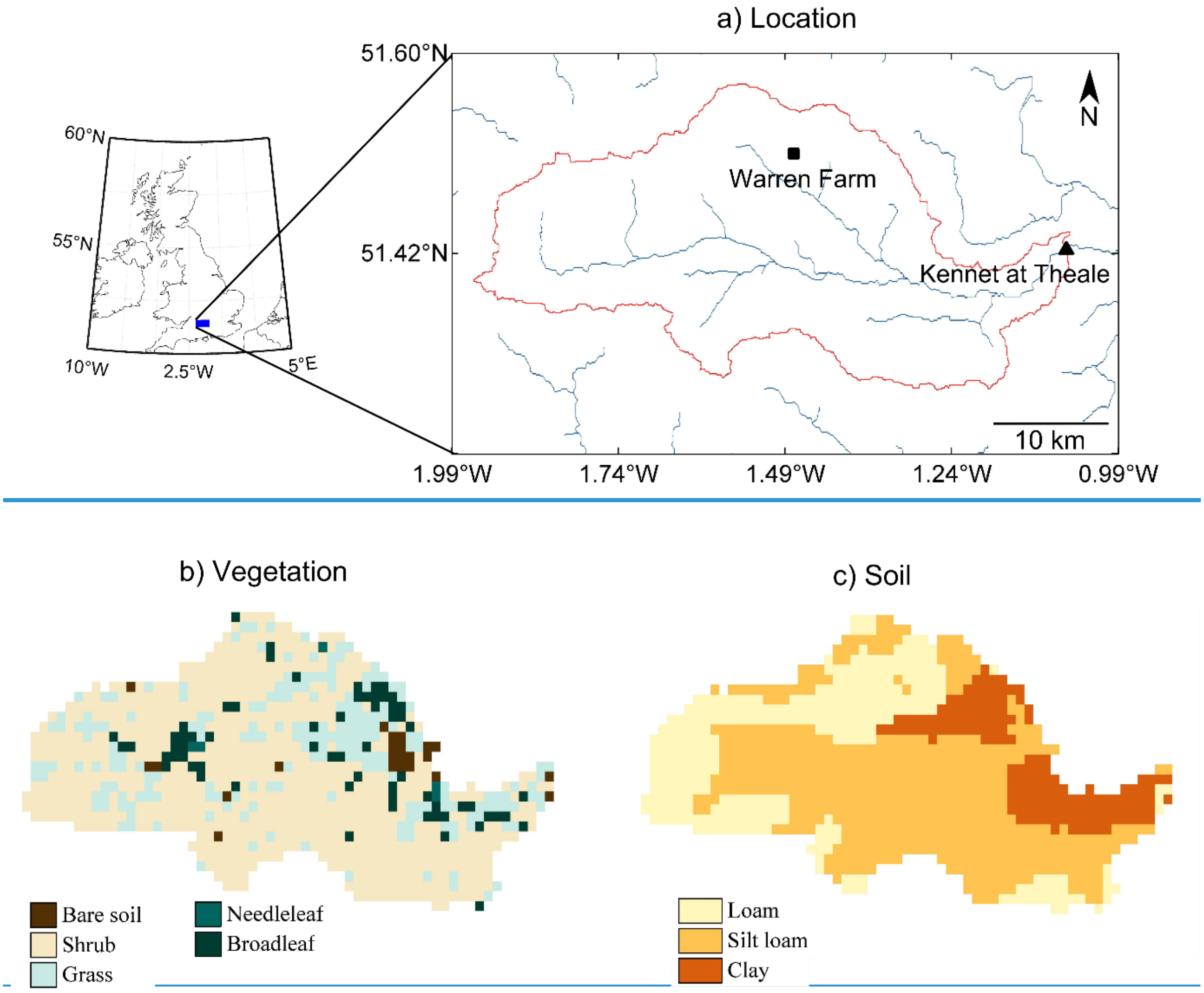

899

900

901

902

903

904 Figure 2. Example of soil profiles collected at Warren Farm during a field campaign in 2015

905 (a), and the two model configurations (b).

906

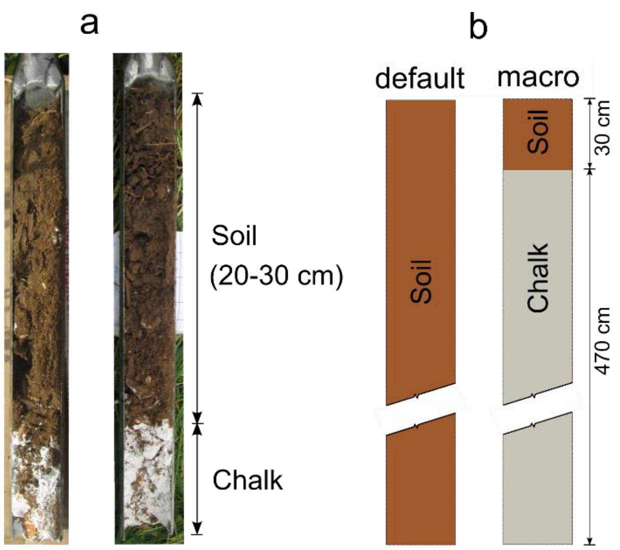

Figure 3. Comparison between observed and simulated (a) soil moisture (θ) and (b) change in soil moisture (Δθ) from the *default* and *macro* configurations at a depth of 2m below land

surface. The shaded areas constructed from 2 soil moisture probes at the Warren Farm site denote the range of observed data in these plots.

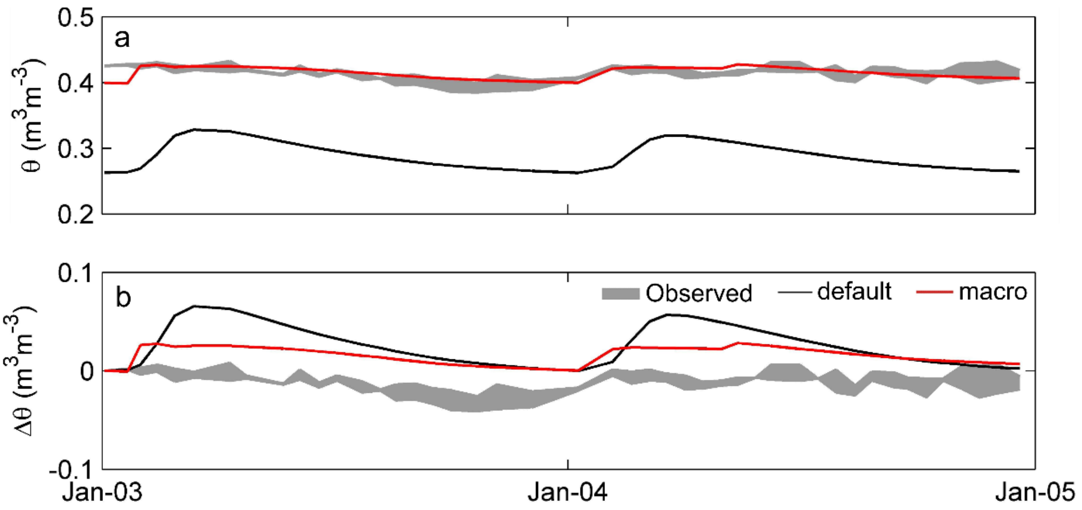

~~Figure 3. Observed and simulated (*default* configuration) volumetric soil moisture from Warren Farm.~~

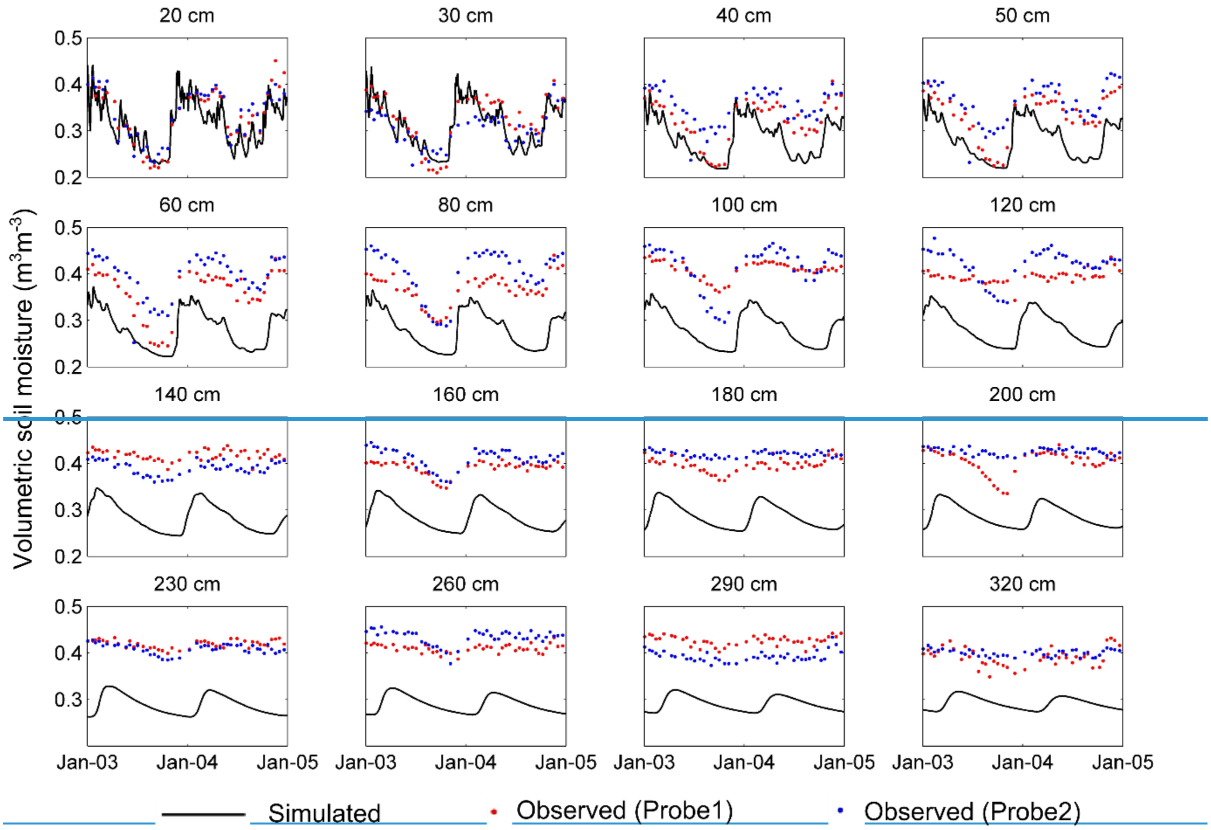

~~Figure 4. Observed and simulated (*macro* configuration) volumetric soil moisture from Warren Farm.~~

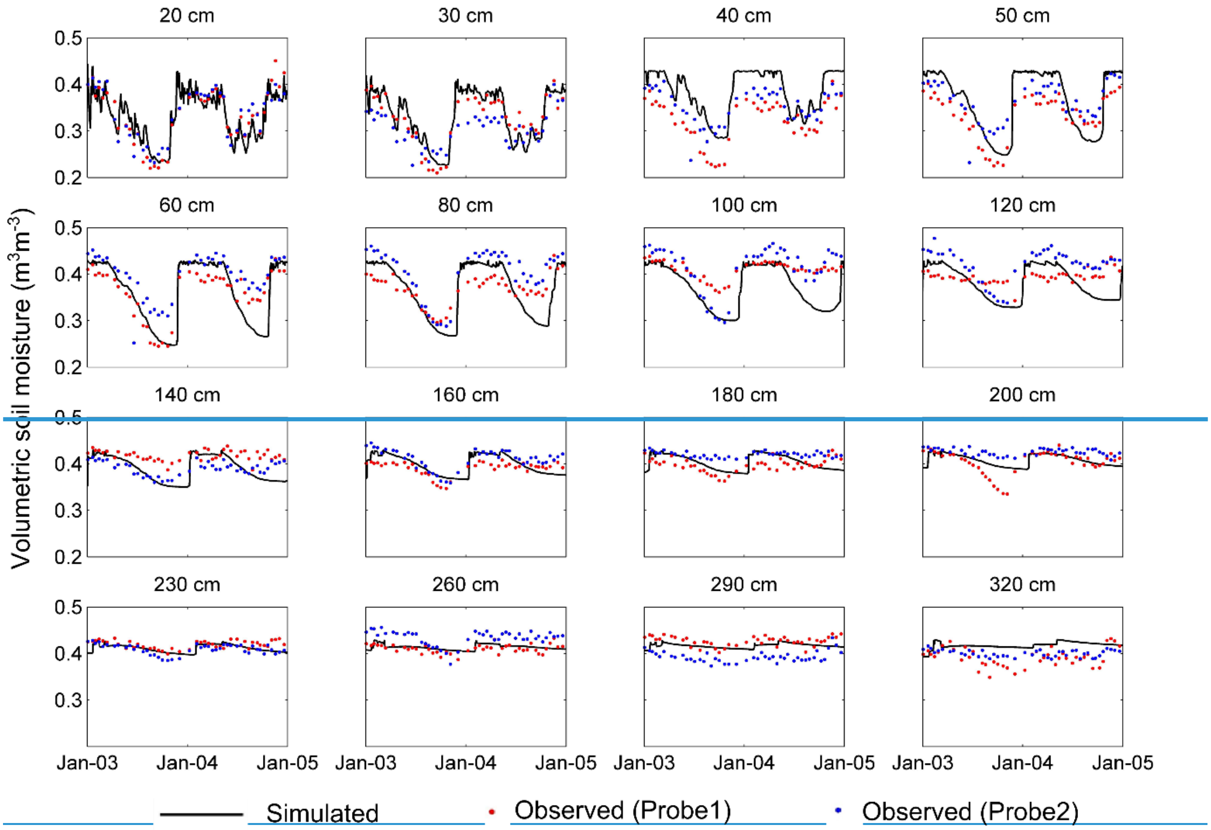

Figure 4. (a) Model performance in reproducing observed and simulated $\Delta\theta$, (b) K_s, (c) S_0 and (d) f_m for various parameter combinations considered in the optimization. Note that except for the *default* and *macro*, the simulation yielding the lowest RMSE (out of 2000 model runs) is presented in this plot.

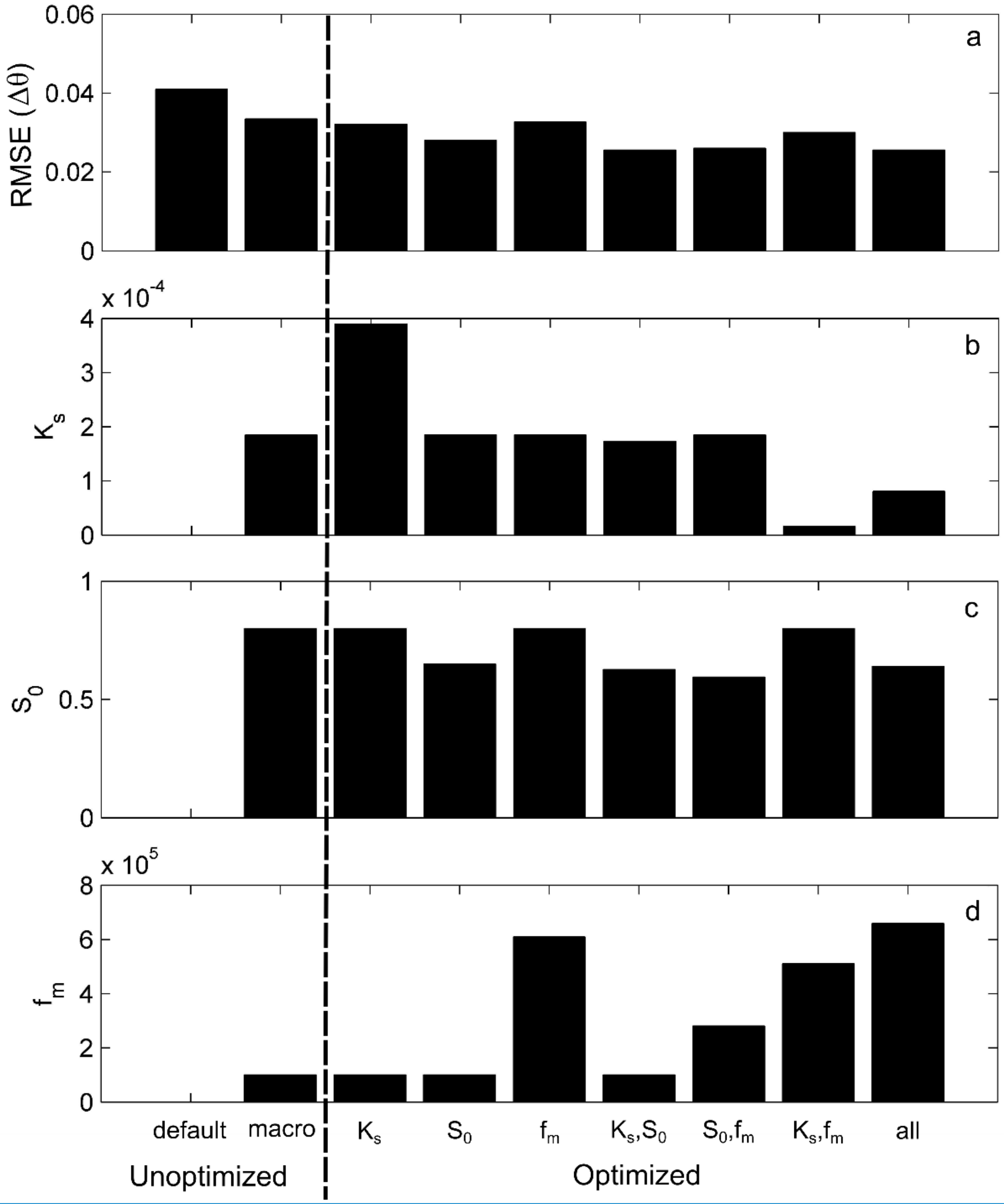

RMSE (Δθ)
0.06
0.04
0.02
0
a
x 10^-4
K_s
4
3
2
1
0
b
S_0
1
0.5
0
c
x 10^5
f_m
8
6
4
2
0
d
default
macro
K_s
S_0
f_m
K_s,S_0
S_0,f_m
K_s,f_m
all
Unoptimized
Optimized

Figure 5. Comparison between observed and simulated $\Delta\theta$ from *default*, *macro* and *macro$_{opt}$* configurations at various depths below land surface. The shaded area, which is constructed from 2 soil moisture probes at the Warren Farm site, denotes the range of $\Delta\theta$.

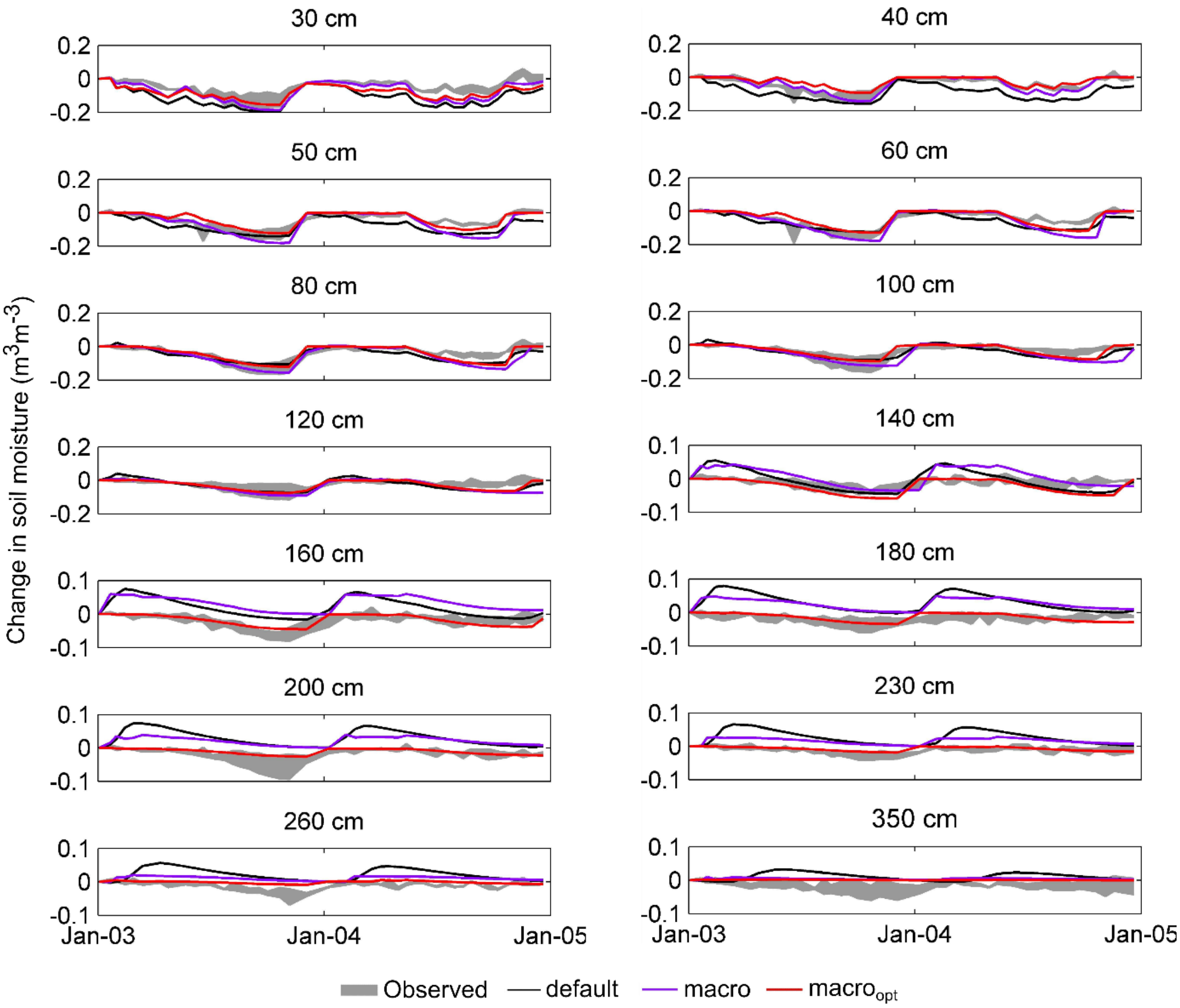

Figure 65. Box plot of relative bias (Δμ) of simulated soil moisture from *default* and *macro* configurations at different depth ranges shown in individual intervals (e.g., 0-30 cm, 30-100 cm, and so on).

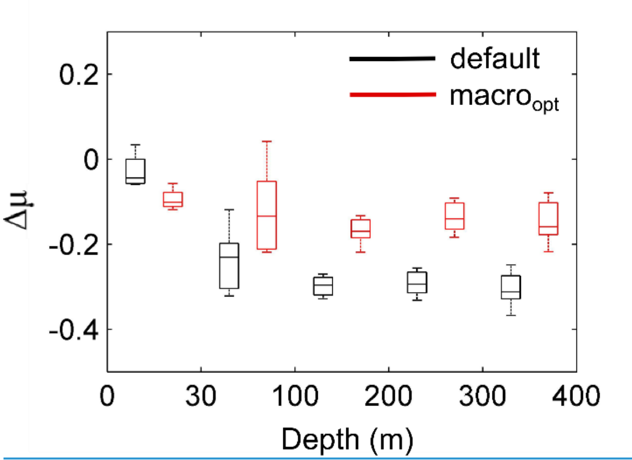

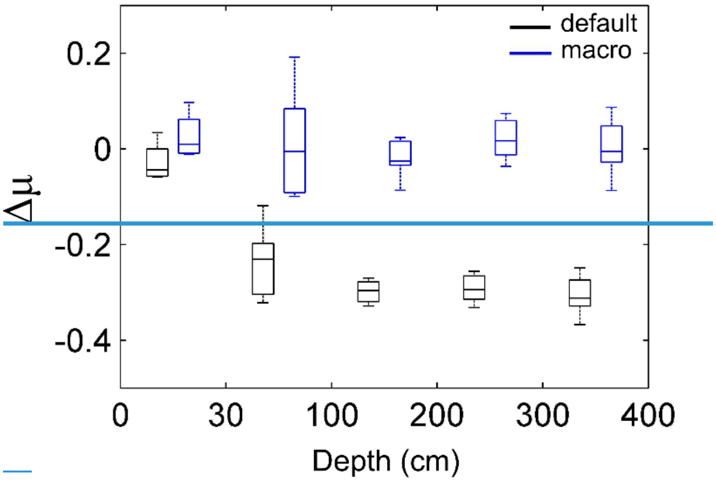

Figure 6. Precipitation (a), daily accumulated downward water flux (w_f, contour lines) plotted over relative saturation (*S*, coloured shading) for *macro* (b), daily accumulated downward water flux plotted over relative saturation for *default* (c), and daily accumulated drainage flux through the bottom boundary simulated by the two model configurations (d) at Warren Farm over the two simulated years (2003-2005).

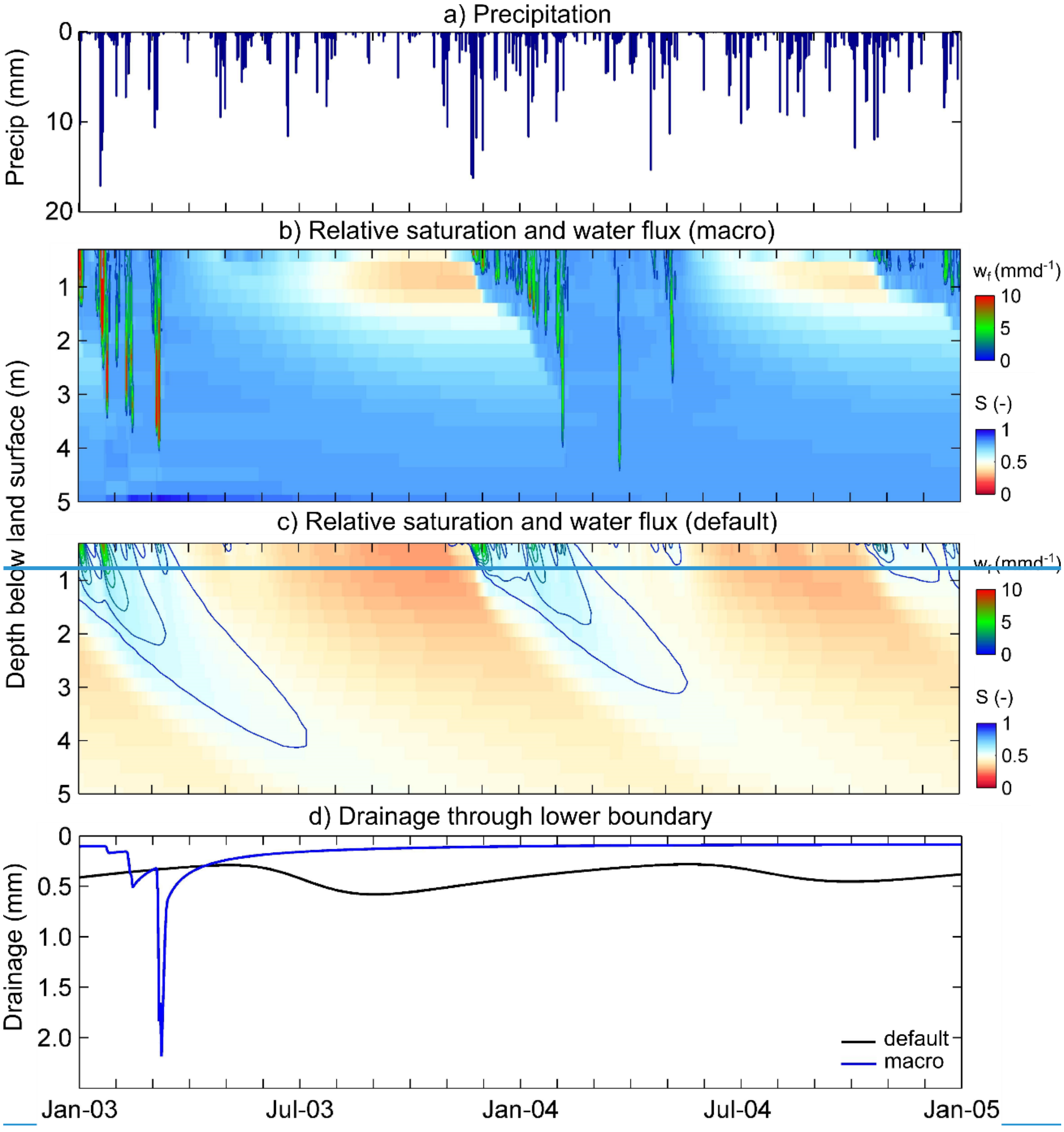

Figure 7. (a) Precipitation and (b) daily sum of drainage through the bottom of the soil column at Warren Farm over the two simulated years (2003-2005).

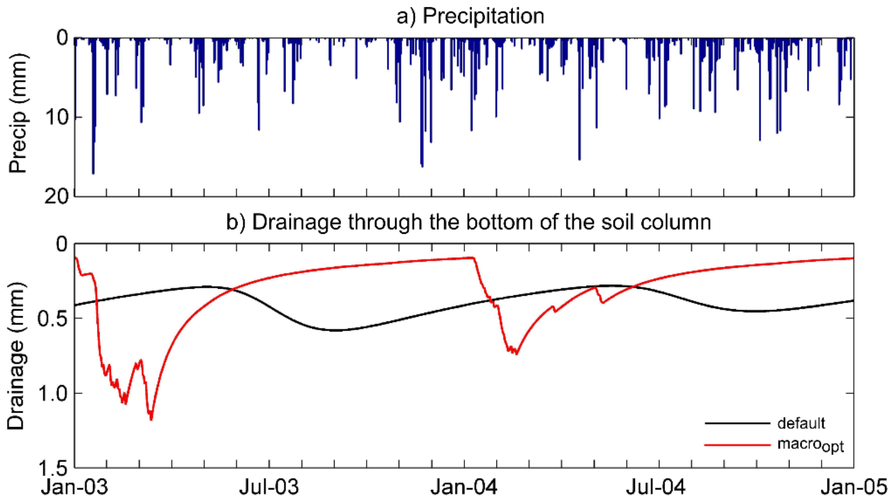

Figure 7. Differences between daily average latent heat flux time series simulated by *default* and *macro* configurations ($LE_{default}$ and LE_{macro}, respectively) at Warren Farm.

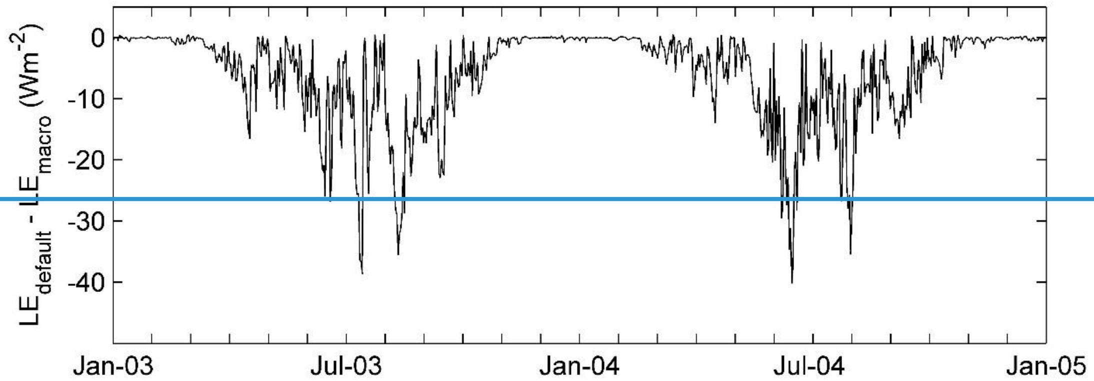

Figure 8. Catchment average 8 day composites of MODIS estimated *LE* (LE_{MOD}) against simulated *LE* from *default* and *macro* configurations ($LE_{default}$ and LE_{macro}, respectively) along

with the linear models fitted for $LE_{default}$ (black line) and LE_{macro} (~~blue~~ red line). The 1:1 line is shown in -grey~~red~~, which represents the perfect fit between LE_{MOD} and simulated LE.

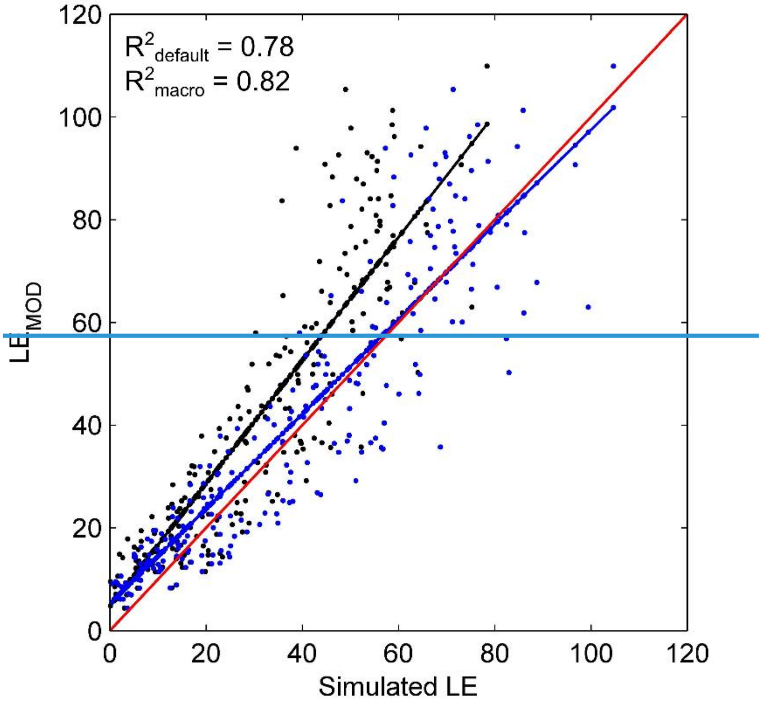

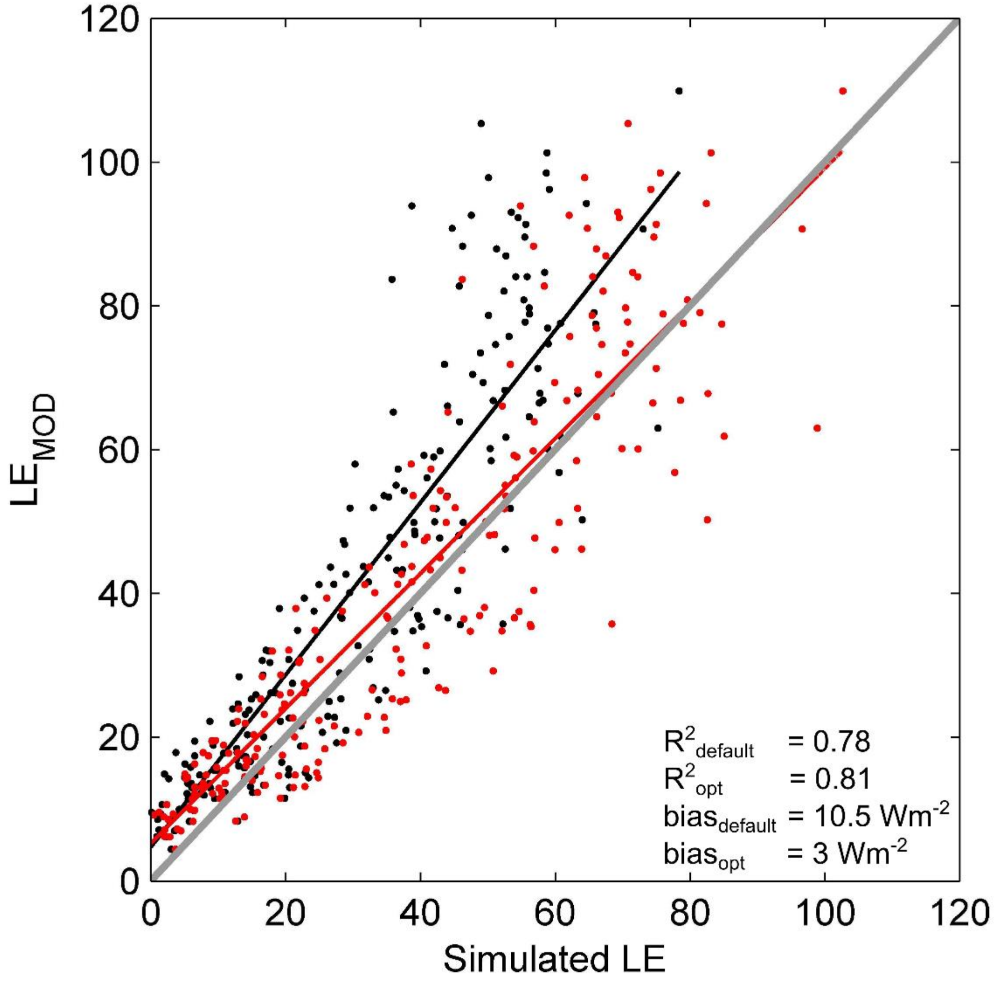

Figure 9. Spatially averaged monthly latent heat flux (*LE*) from MODIS, *default* and *macro*$_{opt}$ configurations over the Kennet catchment.

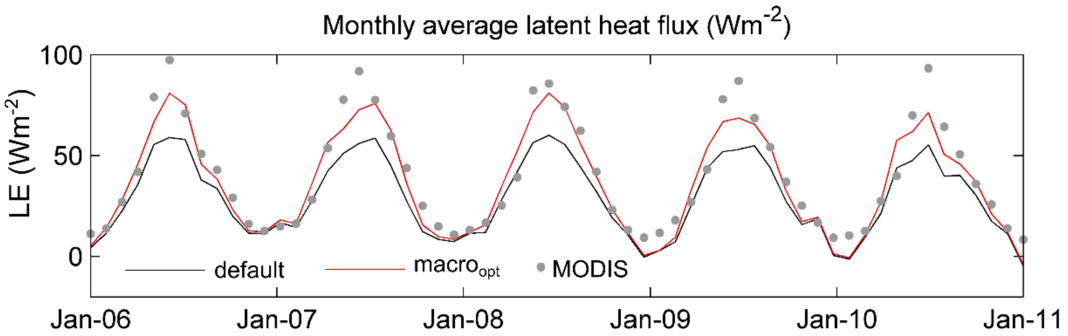

~~Figure 9. Spatially averaged monthly latent heat flux (*LE*) from MODIS, *default*, and *macro* configurations (a), and average (0-100 cm below land surface) daily relative saturation (*S*) from *default* and *macro* configurations (b) over the Kennet catchment.~~

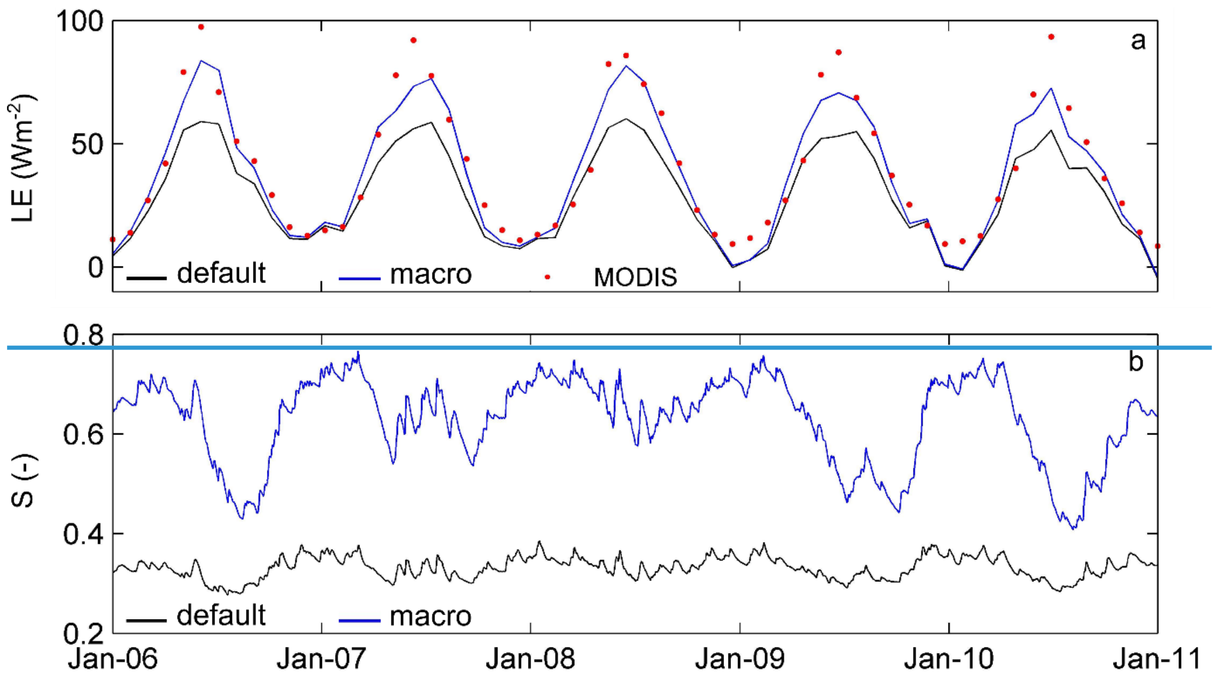

Supplementary materials

Figure S1. Saturation-pressure head relationship (May 2003 - December 2005) at Warren Farm measured fortnightly at 40 cm below land surface. (Source: Ned Hewett, CEH, personal communication).

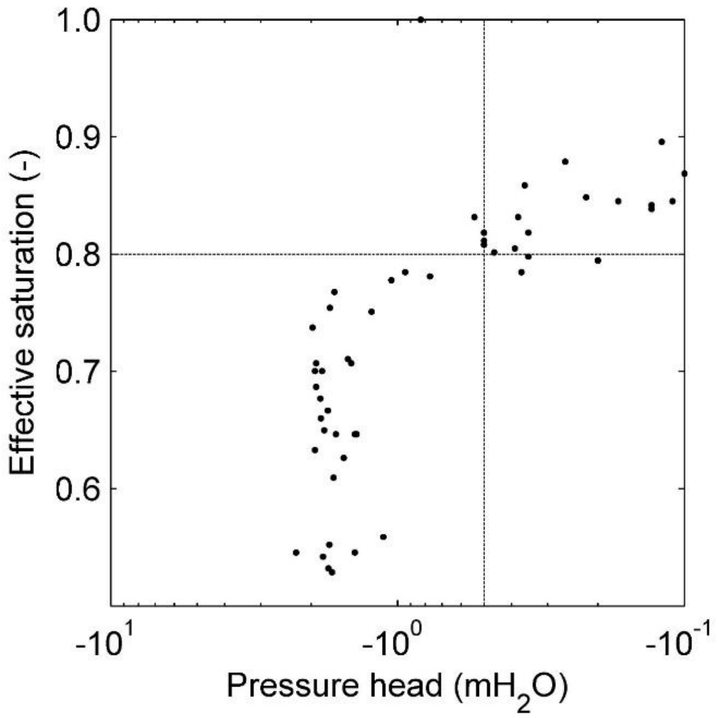

Figure S2. Sensitivity of the BC model parameters on the model performance in simulating $\Delta\theta$. Note that the parameters are considered one-at-a-time (OAT), and the vertical axis have different RMSE ranges.

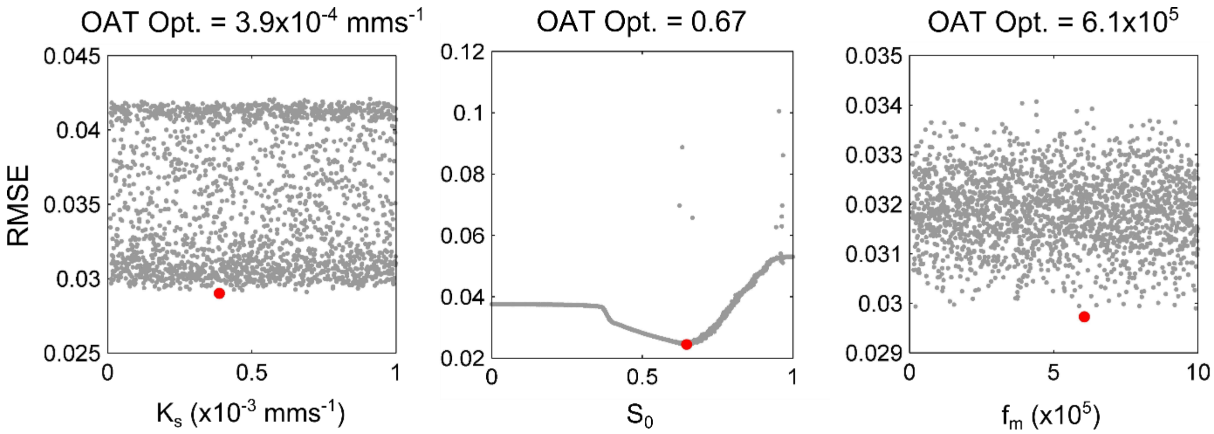
OAT Opt. = 3.9x10-4 mms-1
OAT Opt. = 0.67
OAT Opt. = 6.1x105
RMSE
0.045
0.04
0.035
0.03
0.025
0
0.5
1
Ks (x10-3 mms-1)
0.12
0.1
0.08
0.06
0.04
0.02
0
0.5
1
S0
0.035
0.034
0.033
0.032
0.031
0.03
0.029
0
5
10
fm (x105)